kcal/mol greater stability of **1** over its acyclic isomer, the pentadienyl cation (Table II),[12] is noteworthy. Since the gain in energy on going from 1,3-pentadiene to cyclopentene is only 11 kcal/mol, some favorable electronic features, such as those discussed by Sorensen, must be present in **1**. The pentadienyl radical also is only 10.6 ± 3 kcal/mol less stable than the cyclopent-3-enyl radical.[29]

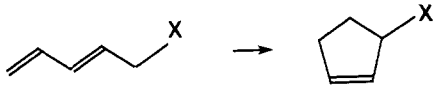

X=H[23b]	-10.7 kcal/mol (expt)
X=· (radical)[28]	-10.6±3 kcal/mol (expt)
X=+ (cation)[3f]	-21 kcal/mol (expt; also see Table 1)

Conclusion

The calculated energy difference of 5-10 kcal/mol between the classical cyclopenten-4-yl cation (**2**) and the cyclopentyl cation (**7**) corresponds to a solvolytic rate ratio (k_6/k_5) of up to 10^7. As the observed rate ratio is only 5-8 (Table III), a rate enhancement up to 10^6 due to anchimeric assistance (k_Δ process) may accelerate solvolyses of **5**; this would explain the high proportion (ca. 95%) of retention of stereochemistry in the homoallylic substitution product. Interpretation of the solvent effects on reactivity using the extended Grunwald-Winstein equation[20] leads to the alternative explanation that solvolyses of **5** and **6** may both be predominantly k_s processes. Stereochemical measurements may be detecting only the onset of the k_Δ process because homoallylic substitution occurs in low yield. This explanation implies that the energy difference between *solvated* ions **2** and **7** is smaller than that calculated for the free ions. Although the bridged cation (**3**) is calculated to be 13 kcal/mol more stable, the classical isomer (**2**) rate enhancements are not observed because bridging lags behind ionization. There also may be a barrier to double-bond participation.

Acknowledgment. Financial support of our work by the Fonds der Chemischen Industrie and the Deutsche Forschungsgemeinschaft is gratefully acknowledged. We thank the Computer Centers at the Universities of Berlin, Erlangen, and Munich for providing generous computer time. We are grateful to G. Llewellyn (Swansea) and W. Zummack (Berlin) for technical assistance and to K. Raghavachari for some of the energies in Table I. This paper is dedicated to Paul D. Bartlett on the occasion of his retirement from Texas Christian University.

Registry No. 1, 63346-43-0; **2**, 81107-93-9; **3**, 81181-41-1; **4**, 54448-32-7; **5**, 36367-85-8; **6**, 3558-06-3.

Supplementary Material Available: Geometries at 6-31G* of ions of **1-3** (3 pages). Ordering information is given on any current masthead page.

(29) McMillen, D. F.; Golden, D. M. *Annu. Rev. Phys. Chem.* **1982**, *33*, 493.

A Study of Long-Range π^*,π^* Interactions in Rigid Molecules Using Electron Transmission Spectroscopy

V. Balaji,[†] L. Ng,[†] K. D. Jordan,*[†] M. N. Paddon-Row,*[‡] and H. K. Patney[§]

Contribution from the Department of Chemistry, University of Pittsburgh, Pittsburgh, Pennsylvania 15260, University of New South Wales, Kensington, New South Wales, Australia 2033, and New South Wales Institute of Technology, New South Wales, Australia 2007. *Received November 17, 1986*

Abstract: Electron transmission (ET) spectroscopy is used to determine the vertical electron affinities of a series of nonconjugated dienes **2-9** and their benzene analogues **11-17** in which the unsaturated moieties are separated by two to six σ bonds. For the compounds in which the benzene or ethylene groups are separated by three or more σ bonds, through-bond interactions are found to be primarily responsible for the observed splittings in the energies of the anion states. In order to explain satisfactorily the energies of the anion states of these compounds, relative to those of the isolated ethylene and benzene molecules, it is necessary to invoke mixing of the π^* orbitals with both the occupied σ and unoccupied σ^* orbitals comprising the connecting σ chains. The large splittings between the symmetric π (π_S) MO's in the photoelectron spectra of **8** and **16** and the absence of such splittings between the π^* MO's in the ET spectra of these compounds provide convincing support for the presence of hyperconjugation between the π_S and bridge orbitals in **8** and **16**.

I. Introduction

This paper is part of a comprehensive program designed to explore orbital interactions through n σ bonds[1,2] (OIT-n-B), involving π and π^* MO's, and how the magnitudes of such interactions depend on the number, n, and the geometry of the relaying σ framework.[2] The techniques of photoelectron spectroscopy (PES)[1d,3] and electron transmission spectroscopy (ETS)[4,5] have been the principal experimental probes in these investigations. The former technique gives the ionization potentials (IP's) and the latter the electron affinities (EA's). In an orbital picture (i.e., within the context of Koopmans' theorem[6]), the IP's and EA's may be associated with the negatives of the energies of the filled and unfilled molecular orbitals, respectively. Hence these experimental methods are ideally suited for the study of intramolecular interactions between remote functional groups.

[†] University of Pittsburgh.
[‡] University of South Wales.
[§] New South Wales Institute of Technology.

(1) (a) Hoffmann, R.; Imamura, A.; Hehre, W. J. *J. Am. Chem. Soc.* **1968**, *90*, 1499. (b) Hoffmann, R. *Acc. Chem. Res.* **1971**, *4*, 1. (c) Gleiter, R. *Angew. Chem., Int. Ed. Engl.* **1974**, *13*, 696. (d) Martin, H.-D.; Mayer, B. *Ibid.* **1983**, *22*, 283.
(2) Paddon-Row, M. N. *Acc. Chem. Res.* **1982**, *14*, 245.
(3) (a) Bock, H.; Ramsey, B. G. *Angew. Chem., Int. Ed. Engl.* **1973**, *12*, 734. (b) Heilbronner, E.; Meier, J. P. In *Electron Spectroscopy: Theory, Techniques, and Applications*; Brundle, C. R., Baker, A. D., Eds.; Academic Press: New York, 1977; Vol. 1.
(4) Sanche, L.; Schulz, G. J. *Phys. Rev. A* **1968**, *5*, 1972.
(5) Jordan, K. D.; Burrow, P. D. *Acc. Chem. Res.* **1978**, *11*, 341.
(6) Koopmans, T. *Physica* **1934**, *1*, 104.

0002-7863/87/1509-6957$01.50/0

In previous work, PES was used to determine the IP's of the series of rigid dienes (**1–10**),[7a–g] their benzene annelated analogues

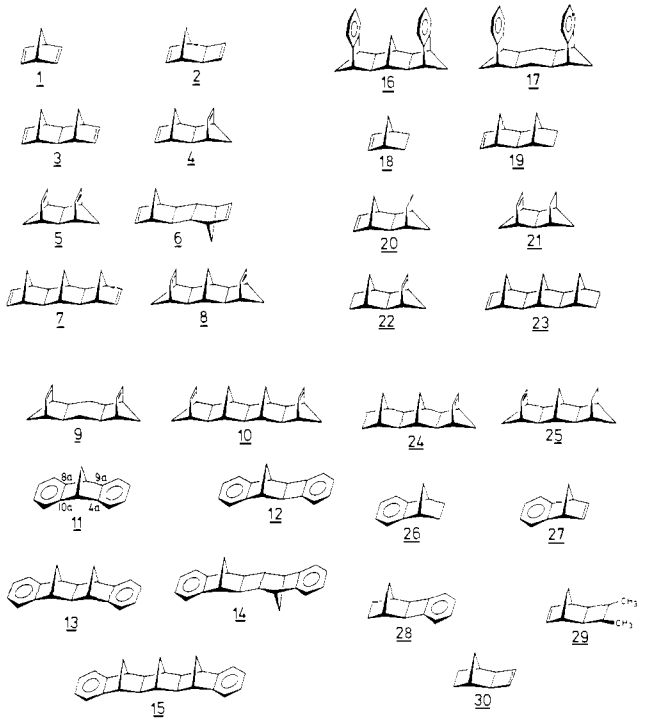

(**11**, **13–17**),[7e] and the associated monoenes and monobenzenes (**18–28**, **30**).[7] ETS results for **1**, **3–5**, and **18–22** have also been reported in a preliminary communication.[8] In the present work the ETS studies are extended to include the dienes **2**, **6–9**, the corresponding dibenzo analogues **11–17**, and also the mono-π systems **24–30**, thereby allowing for a systematic analysis of through-bond (TB) interactions in both the filled and unfilled orbitals. In order to set the stage for the new studies, the main findings of the prior investigations are first summarized.

The PES studies on the dienes **2**, **3**, **6**, and **7** showed that OIT-n-B between the π MO's are attenuated relatively slowly with increasing n. Thus the splitting energies, π–ΔIP, between π_+ and π_- MO's[9] in **2** (n = 3), **3** (n = 4), **6** (n = 5), and **7** (n = 6) are 1.1,[7b] 0.87,[7c] 0.43,[7e] and 0.32 eV,[7f] respectively.

The trends in the ionization potentials (IP's) also substantiate Hoffmann's prediction[1a,2] that TB interactions should depend on the conformation of the framework, being maximal for a coplanar all-trans arrangement of the σ bonds as in dienes **2**, **3**, **6**, and **7** and smaller in cis–trans arrangements as in **4**. For example, the π-ΔIP value for **3** (0.87 eV)[7c] is much larger than that of **4** (0.44 eV).[7d] The TB contribution to the π-ΔIP value for **5**, having the cis–cis arrangement of relaying σ bonds, is predicted to be even smaller than that for **4**. However, it is found that the π-ΔIP of **5** is considerably larger than that of **3**. This result is attributed to the presence of large through-space (TS) interactions in **5**.[7d]

The PE spectra of the dienes **8** and **10** revealed splitting energies of 0.52[7f] and 0.27 eV,[7g] respectively. These values are much too large to be accounted for exclusively in terms of OIT-6-B-in **8** and OIT-8-B in **10**. It has been proposed that the observed splittings are caused largely by hyperconjugative interactions between the π MO's and the orbitals of the intervening methylene groups.[10] This interaction, termed laticyclic hyperconjugation,[10] is illustrated below for **8** and **10**. In diene **8**, the π_- MO is much

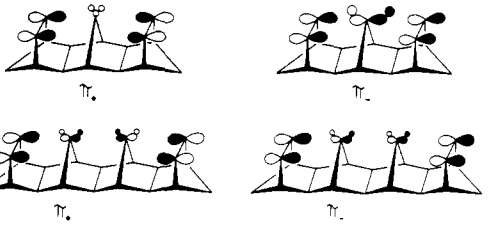

more affected by this type of mixing than is π_+ on account of the superior overlapping ability of the antisymmetric CH_2 pseudo-π MO compared with the symmetric CH_2 MO (which can mix only weakly with π_+). In diene **10**, symmetry-adapted combinations of CH_2 pseudo-π MO's can be formed which can mix with π_+ and π_-. Again overlap considerations suggest that π_- should be more affected than π_+ but that the difference should be less pronounced than in **8**.

The PE spectra of the benzene-annelated derivatives of the above dienes also show sizable splittings of the π orbitals due to interactions through the connecting C–C σ bonds or through laticyclic hyperconjugation.[7e] The splittings are larger for the orbitals derived from the highest occupied molecular orbital (HOMO) of the benzene molecules than for those from the second highest occupied orbital (SHOMO). The phases of the HOMO (π_S) and SHOMO (π_A) and the corresponding unoccupied orbitals of the substituted benzenes are shown below.

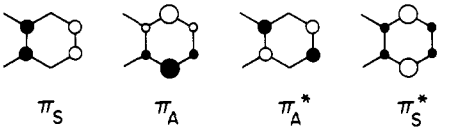

The "S" and "A" subscripts are used to indicate whether the orbitals are symmetric or antisymmetric with respect to the symmetry plane retained in the derivatives. The π_S and π_A MO's are degenerate in benzene but are appreciably split in *o*-xylene and in **11–17** and **26–28**. The splitting between the π_A* and π_S* orbitals of *o*-xylene and related compounds, however, is generally quite small.[12] The ratio of ΔIP for each of the dienes **1**, **3**, and **6–8** to π_S-ΔIP of the corresponding benzene analogue, i.e., **11**, **13–16**, was found to be roughly constant, ranging from 1.2 to 1.6, irrespective of the origin of the splitting (i.e., TS, TB, or laticyclic hyperconjugation).[7e] A simple one-electron zero differential overlap model, in which the splitting energies depend on the squares of the π orbital coefficients of the interacting carbon atom (1/2 for a vinylic C and 1/4 for a benzene C atom in the π_S HOMO), predicts a ratio of 2.0. STO-3G calculations give a value of 1.9 for the ratio π-ΔIP(**3**)/π_S-ΔIP(**13**). Part of the remaining

(7) (a) **1**, **18**: Heilbronner, E.; Martin, H.-D. *Helv. Chim. Acta* **1972**, *55*, 1490. (b) **2**, **30**: Brogli, F.; Eberbach, W.; Haselbach, E.; Heilbronner, E.; Hornung, V.; Lemal, D. M. *Ibid.* **1973**, *56*, 1933. (c) **3**, **19**, **20**, **22**: Paddon-Row, M. N.; Patney, H. K.; Brown, R. S.; Houk, K. N. *J. Am. Chem. Soc.* **1981**, *103*, 5575. (d) **4**, **5**: Martin, H.-D.; Schwesinger, R. *Chem. Ber.* **1974**, *107*, 3143. (e) **6**, **11**, **13–17**: Paddon-Row, M. N.; Patney, H. K.; Peel, J. B.; Willet, G. D. *J. Chem. Soc., Chem. Commun.* **1984**, 564. (f) **7–9**, **24**, **25**: Jorgensen, F. S.; Paddon-Row, M. N.; Patney, H. K. *Ibid.* **1983**, 573. (g) **10**: Jorgensen, F. S.; Paddon-Row, M. N. *Tetrahedron Lett.* **1983**, *24*, 5415. (h) **21**: Prinzbach, H.; Sedelmeier, G.; Martin, H.-D. *Angew. Chem., Int. Ed. Engl.* **1977**, *16*, 103. (i) **26**, **27**: Domelsmith, L. N.; Mollere, P. D.; Houk, K. N.; Hahn, R. C.; Johnson, R. P. *J. Am. Chem. Soc.* **1978**, *100*, 2959. (j) **28**: Brown, R. S.; Paddon-Row, M. N., unpublished.

(8) Balaji, V.; Jordan, K. D.; Burrow, P. D.; Paddon-Row, M. N.; Patney, H. K. *J. Am. Chem. Soc.* **1982**, *104*, 6849.

(9) In this paper, π_+ refers to the bonding combination of the localized π orbitals, π_A and π_B, i.e., $\pi_+ = \pi_A + \pi_B$, whereas π_- refers to the antibonding combination, i.e., $\pi_- = \pi_A - \pi_B$. For double bonds separated by an even number of σ bonds, as in **1** and **3**, the π_+ and π_- orbitals are distinguished by a reflection plane, whereas those separated by an odd number of σ bonds, as in **2** and **6**, are distinguished by a (pseudo) C_2 symmetry axis as can be seen from the

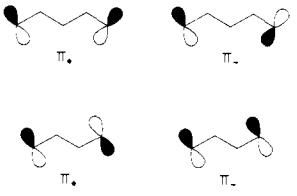

This classification can also be used to describe how the σ orbitals behave under these symmetry operations as can be seen from Figure 4.

(10) Paddon-Row, M. N. *J. Chem. Soc., Perkin Trans. 2* **1985**, 257.

(11) Brogli, F.; Giovanni, E.; Heilbronner, E.; Schurter, R. *Chem. Ber.* **1973**, *106*, 961.

(12) Jordan, K. D.; Michejda, J. A.; Burrow, P. D. *J. Am. Chem. Soc.* **1976**, *98*, 1295.

discrepancy may be due to the fact that (counting the bonds in the rings themselves) the σ chains are actually longer in the benzene annelated compounds than in the corresponding dienes.

The earlier ETS studies of **3–5** showed that the π_+* and π_-* orbitals tend to be shifted less in energy by TB interactions than are the π_+ and π_- orbitals.[8] However, the TB interactions shift the π_+* and π_-* orbitals in opposite directions, while they cause the π_+ and π_- orbitals to be shifted in the same direction, with the net result that the splittings between the π* MO's are comparable to those between the π MO's. In order to explain the shifts in the π* orbitals it was necessary to invoke the mixing with both the σ and σ* MO's, whereas the splittings between the π orbitals could be adequately explained with a model including only mixing with filled σ MO's.[2,7c]

The ETS studies carried out here will supplement the earlier work in that systems with double bonds separated by three, five, and six bonds will be examined, as will several of the benzene annelated analogues. ETS measurements on compounds **8**, **9**, **16**, and **17** provide a particularly stringent test of the laticyclic hyperconjugation theory:[10] by dint of symmetry, laticyclic interactions of the type depicted above should be absent in the π* orbitals of **8** and for the π_A* orbitals of **16**.

Although hyperconjugative interactions involving π* MO's and orbitals of the CH_2 bridging groups are possible (shown in the inset), the results of the ETS measurements as well as calculations

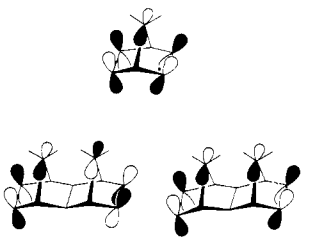

on a series of model compounds indicate that they are much less important than the C–C σ TB interactions. Consequently, they will be neglected in the remainder of the paper.

Studies on TB interactions are timely in light of recent rate measurements of photoinduced electron transfer in rigid systems such as **31**[13] and of thermal electron transfer in radical anions of compounds such as **32**.[14] It was found that the electron transfer

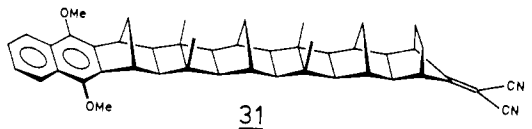

31

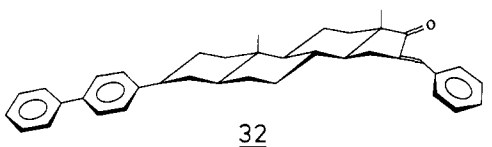

32

is surprisingly fast, taking place within 2×10^{-9} s, even in **31** in which the center-to-center separation of the two chromophores is ca. 15 Å.[13c] This raises the question: to what extent is the electron transfer in such compounds promoted by coupling through the σ network? ETS investigation of compounds such as **1–17** cannot provide a direct answere to this question because, owing to electron autoionization, the gas-phase anions have lifetimes much shorter than the transfer rates found in the solution studies. However, they can provide insight into the relative importance of π*/σ and π*/σ* mixing for functional groups separated by 4–8 Å. Such information, which is related to the electron coupling (transfer) integral,[15] is valuable for assessing the plausibility of long-range electron-transfer processes involving a through-bond mechanism.

Section II of this paper presents a brief review of the technique of ETS. The results on the dienes and benzene compounds are presented in sections III and IV, respectively. The distance dependence of OITB is discussed in section V, and the implications that the PES and ETS data for these compounds have for the mechanisms of long-range intramolecular electron transfer are discussed in section VI. Concluding remarks are given in section VII.

II. Electron Transmission Spectroscopy

The technique of ETS has been described in detail elsewhere,[4,5] and only a brief summary is given here. In ETS a beam of monoenergetic electrons is transmitted through the vapor of the compound of interest. Electrons which lose momentum in the forward direction are discriminated against by means of a retarding region located between the collision cell and the collector. At those energies corresponding to electron capture, there is a rapid change in the transmitted current. In the format utilized here the derivative with respect to energy of the transmitted current is measured as a function of the incident electron energy. We associate the most probable attachment energies or vertical electron affinities (EA) with the inflection points, marked by vertical lines on the spectra. The assumptions made with this association are discussed elsewhere.[16] The full-width at half-maximum resolution is better than 0.05 eV, and calibration of the energy scale is accomplished either by reference to the beam onset or reference to the structure in the well-characterized $^2\Pi_g$ ground-state anion of N^2.[17] The absolute energies of the various features in the ET spectra are thus determined to within 0.05 eV.

Normally ET spectra are obtained under high-retarding conditions, under which nearly all electrons which have lost momentum in the forward direction are rejected. In this mode of operation the resulting spectrum corresponds closely to a total scattering cross-section measurement. For some of the molecules examined in this study, spectra obtained under low-retarding conditions are also reported. In this mode of operation one collects all electrons except those elastically scattered into a small cone about a scattering angle of 180°.[18] This essentially permits one to obtain a measurement of the 180° elastic scattering cross section. The principal advantages of the low-retarding approach are that for some molecules it provides enhanced visibility of vibrational structure and resolution of features due to two closely spaced anion states which would appear as a single broad peak in the total scattering cross section. Unless stated otherwise, it is assumed that the high-retarding approach has been used to obtain the spectra.

Although the full-width at half-maximum resolution is about 0.05 eV, it does not necessarily follow that the ET spectra will show two distinct peaks whenever the splitting between two anion states exceeds 0.05 eV. The reason for this is that the individual peaks may have widths much greater than 0.05 eV. If the lifetime of anion state is sufficiently long that appreciable motion of the nuclei can occur before electron detachment, then well-resolved structure due to vibrational excitation will appear. The ground-state anion of benzene provides such an example. On the other hand, for anions with very short lifetimes, only a very broad feature with a width determined primarily by the detachment rate is observed. Of particular interest is the intermediate case in which the lifetime is sufficiently short that no (or only very weak) structure due to nuclear motion is observed but sufficiently long that the overall width of the anion state is determined primarily from that of the Franck-Condon envelope rather than from the

(13) (a) Hush, N. S.; Paddon-Row, M. N.; Cotsaris, E.; Oevering, H.; Verhoeven, J. W.; Heppener, M. *Chem. Phys. Lett.* **1985**, *117*, 8. (b) Warman, J. M.; de Haas, M. P.; Paddon-Row, M. N.; Cotsaris, E.; Hush, N. S. *Nature (London)* **1986**, *320*, 615. (c) Oevering, H.; Paddon-Row, M. N.; Oliver, A. M.; Cotsaris, E.; Verhoeven, J. W.; Hush, N. S. *J. Am. Chem. Soc.*, in press.

(14) Calcaterra, L. T.; Closs, G. L.; Miller, J. R. *J. Am. Chem. Soc.* **1983**, *105*, 670.

(15) Hush, N. S. *Coord. Chem. Rev.* **1985**, *64*, 135.

(16) Burrow, P. D.; Michejda, J. A.; Jordan, K. D. *J. Chem. Phys.* **1987**, *86*, 9.

(17) Schulz, G. J. *Rev. Mod. Phys.* **1983**, *45*, 423.

(18) Johnston, A. R.; Burrow, P. D. *J. Electron Spectrosc. Relat. Phenom.* **1982**, *25*, 119.

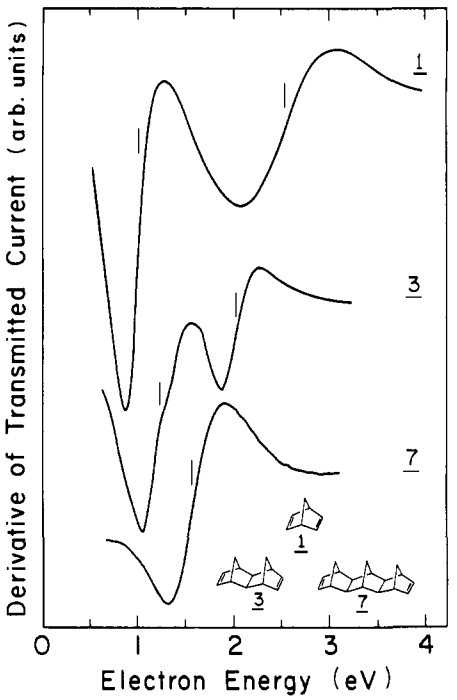

Figure 1. Derivative of the transmitted curent as a function of the electron energy in compounds **1**, **3**, and **7**.

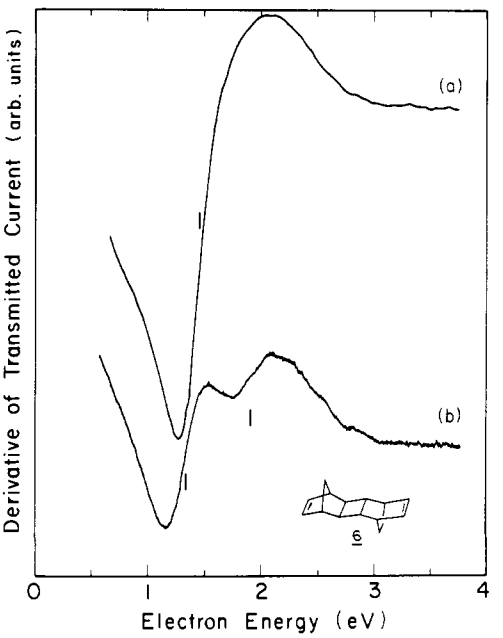

Figure 2. Derivative of the transmitted current as a function of electron energy in **6**. The spectra labeled (a) and (b) are obtained under high- and low-retarding conditions, respectively.

detachment rate. The moleucles studied here appear to fall into this intermediate category. Since the Franck-Condon envelopes have widths of the order of 0.4–0.5 eV, in general it will not be possible to resolve peaks due to two close-lying anion states unless they are separated by several tenths of an eV. However, even when two states give rise to a single feature in the ET spectrum, it may still be possible to obtain a crude estimate of the splitting from comparison of the line width with those of the isolated anion states of related compounds.

III. Dienes

A. ETS Spectra. The ET spectra of compounds **1**, **3**, and **7** in which the two ethylene groups are separated by two, four, and six σ bonds, respectively, are presented in Figure 1. The spectra of **1** and **3** are from ref **19** and **8**, respectively, and that of **7** is reported here for the first time. In norbornadiene (**1**) the two double bonds are sufficiently close (ca. 2.5 Å) that through-space interactions make the major contribution to the 1.52-eV splitting observed between the π_+* and π_-* anion states. In **3** and **7** the distance between the double bonds is sufficiently large (ca. 5 and 8 Å, respectively) that through-space interactions should be negligible (i.e., less than a few hundredths of an eV.). Hence, the 0.8-eV splitting found[8] between the anion states (as well as between the cation states) of **3** must derive from OIT-4-B as was discussed in the Introduction.

The high-retarding spectrum of **2** has a single feature at 1.56 eV with a width of 0.5 eV, comparable to that found in the monoenes. If there are two anion states near 1.56 eV it is unlikely that they could be separated by more than 0.1–0.2 eV. This result is most puzzling since the theoretical calculations, using the STO-3G basis set and assuming the validity of Koopmans' theorem (KT), which work quite well for the other systems, predict a 0.9-eV splitting between the two anion states of this compound. Also the corresponding benzene analogue, **12**, shows an appreciable splitting between the anion states. It is unlikely that the sample could have decomposed while the spectrum was run, since **2** is thermally stable for several hours at 120 °C, and it gives a normal PE spectrum.[7b] One factor which could be important in causing the splitting between the π_+* and π_-* anion states of **2** to be considerably less than that expected based on the TB model and STO-3G calculations is the involvement of long-range TS interactions. Such interactions would be more important for the anion than cation states and would act so as to decrease the π_+*, π_-* splitting. Indeed, calculations with the more extended 3-21G basis set give a π_+*,π_-* splitting of only 0.53 eV, while giving a π_+,π_- splitting nearly the same as that obtained with the STO-3G basis set. With an even more extended basis set the splitting between the anion states could be even smaller. (We did not explore this possibility, because with very diffuse functions in the basis set, calculations on temporary anions are prone to "collapse" to the neutral molecule plus "free" electron.) In any case, these calculations support the idea that the opposing effects of TB and TS interactions give rise to a relatively small net splitting between the π_+* and π_-* anion states of **2**, consistent with the existence of a single feature in the ET spectrum of this compound. This leaves open the question as to why splittings are seen in the ET spectrum of the corresponding dibenzo compound. One possible explanation is that the long-range TS interactions are much less important in the dibenzo compound than in the diene. This could happen if the lifetime of the anion states of the former were appreciably greater than those of the latter compound. The spatial extent of the anion wave functions should, in general, increase with decreasing lifetime. It is not possible to test this hypothesis with crude calculations of the type employed here.

The high-retarding spectrum of **6** (see Figure 2) has a broad feature (width 0.9 eV) centered at 1.5 eV, apparently due to both the π_+* and π_-* anion states. Since this feature is about 0.4 eV broader than those in the ET spectra of the various monoenes and the dienes, **3**, and **7**, it would appear that the two anion states are split by a few tenths of an eV. This is confirmed by the spectrum obtained under low-retarding conditions, which gives two well-resolved peaks at 1.35 and 1.92 eV. A detailed discussion of the difference between the low-retarding and high-retarding spectra of this compound will be given in the next section.

The high-retarding spectrum of **7** shows only a single broad structure at 1.60 eV, which is precisely the energy of the peak in the ET spectrum of the monoenes **24** and **25** but 0.18 eV below the anion state of ethylene. The width of this feature is 0.75 eV, about 0.25 eV greater than the widths of the anion states of **3**. This suggests that the two anion states of **7** are split by about 0.2–0.3 eV. The low-retarding spectrum of **7** reveals a large feature at 1.5 eV with a very weak shoulder near 1.75 eV, consistent with an 0.2–0.3 eV splitting.

The ET spectra of **8** and **9** each have only a single broad peak at low energy and are not reproduced here. (For these two compounds there was insufficient sample to permit determination of the low-retarding spectra.) In both cases the center of the peak

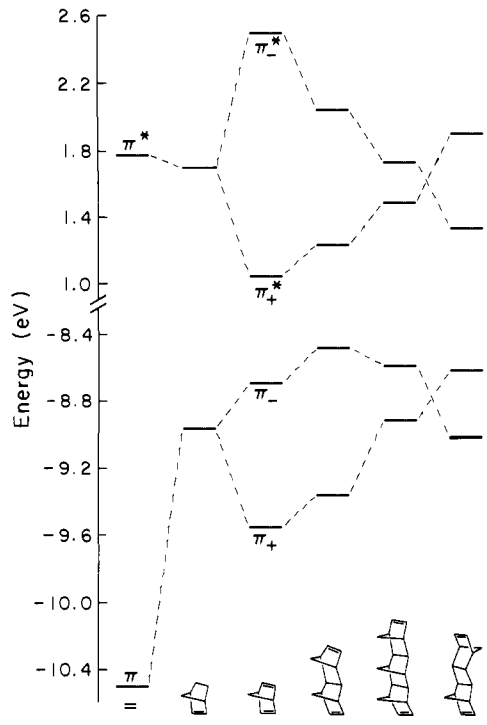

Figure 3. Correlation diagram giving the negatives of the vertical IP's and EA's of **1**, **3**, **6**, **7**, **18**, and ethylene.

Table I. Experimental Vertical Ionization Potentials[a] and Electron Affinities[b]

molecule	IP (eV)	EA (eV)	molecule	IP (eV)	EA (eV)
ethylene	10.51	−1.78	**26**	8.45	−1.12
benzene	9.25	−1.12		8.95	
18	8.97	−1.70	**27**	8.32	−0.92
19	8.85	−1.65		9.03	−1.28
20	8.78	−1.65		9.35	−2.01
21	8.60	−1.68	**28**	8.65	−1.05
22	8.65	−1.51		9.03	
24	8.47	−1.47	**29**		−1.70
25	8.51	−1.50	**30**	9.00	−1.73

[a] The experimental IP's are from the following references: ethylene, ref 32; benzene, ref 33; **18**, ref 79; **19**, **20**, and **22**, ref 7c; **21**, ref 7h; **24** and **25**, ref 7f; **26** and **27**, ref 7i; **28**, ref 7j; **30**, ref 7b. [b] The experimental EA's are from the following references: ethylene, ref 5; benzene, ref 16; **18–22**, ref **8**; **24–30**, present study.

is close to that of the monoene **25**, and the width of the peak is about 0.2 eV greater than those due to the anion states in **3–5** (or in the monoene **25**). Again this is indicative of a small (0.1–0.2 eV) splitting between the two anion states. There is no evidence of an increased splitting between the anion states of **8** compared to those of **9**. Thus, in contrast to the situation for the cation states,[7f] laticyclic hyperconjugation is negligible in the anion states of **8**. This finding is consistent with the symmetry considerations discussed in the Introduction and with the results of calculations on model systems. For example, STO-3G calculations on a model comprised of two ethylenes oriented as in **8** together with a methane in place of the bridging methylene yields a π_+^*/π_-^* splitting of only 0.03 eV in contrast to a π_+/π_- splitting of 0.39 eV.

B. Model of Through-Bond Interactions. The IP's and EA's for **1**, **3**, **6**, and **7** are summarized in the correlation diagram given in Figure 3. For comparative purposes, results have been also included for ethylene and norbornene (**18**). The IP's and EA's of these species as well as those of the other compounds studied here are summarized in Tables I and II. To interpret the trends shown in the correlation diagram, it is helpful to expand the model introduced in ref 2, 7c, and 8. In this model one starts with "pure"

Table II. Vertical Ionization Potentials[a] and Electron Affinities[b]

molecule	IP (eV)	π ± π splitting[a-c]	EA (eV)	π* ± π* splitting[c-e]
1	8.69 (b_1)		−1.04 (b_2)	
	9.55 (a_1)	0.86 (0.80)	−2.56 (a_2)	1.52 (1.70)
3	8.48 (b_1)		−1.25 (b_2)	
	9.35 (a_1)	0.87 (0.89)	−2.05 (a_2)	0.80 (0.81)
4	8.46 (a′)		−1.26 (a″)	
	8.90 (a′)	0.44 (0.52)	−2.03 (a″)	0.77 (0.54)
5	8.08 (b_1)		−1.05 (b_2)	
	9.34 (a_1)	1.26 (1.55)	−2.50 (a_2)	1.45 (1.29)
6	8.60 (a_g)		−1.35 (b_g)	
	9.03 (b_u)	0.43 (0.27)	−1.92 (a_u)	≈0.60 (0.35)[f]
7	8.58 (b_1)		−1.50 (b_2)	
	8.90 (a_1)	0.32 (0.31)	−1.75 (a_2)	0.25 (0.22)[f]
8	8.24 (b_1)		−1.53 (b_2,a_2)	
	8.76 (a_1)	0.52 (0.51)		S (0.03)
9	8.62 (b_1)		−1.63 (b_2,a_2)	
	8.80 (a_1)	0.18 (0.20)		S (0.05)
11	8.17 (b_1)		−0.67 (b_2)	
	8.76 (a_2,a_1)	0.60 (0.66)	−0.88 (a_1)	0.98 (0.93)
	9.05 (b_2)	0.29 (0.14)	−1.55 (b_1)	0.67 (0.67)
			−1.65 (a_2)	
12			−0.59 (a″)	
			−0.69 (a′)	0.48 (0.45)
			−1.07 (a″)	
			−1.29 (a′)	≤0.60 (0.45)
13	8.10 (b_1)		−0.90 (a_1,b_2)	≈0.5 (0.37)
	8.66 (a_1)	0.56 (0.47)		
	8.80 (a_2)		−1.43 (b_1,a_2)	≤0.5 (0.29)
	8.94 (b_2)	0.14 (0.16)		
14	8.26 (a_g)	0.31	−1.19 (a_u,b_g)	S
	8.57 (b_u)			S
	8.95 (a_u,b_g)	≈0		
15	8.23 (b_1)		−1.25 (a_1,b_2 / b_1,a_2)	S
	8.49 (a_1)	0.26		S
	8.81 (a_2,b_2)	≈0		
16	7.98 (b_1)		−0.93 (a_1,b_2 / b_1,a_2)	S
	8.36 (a_1)	0.38		S
	8.81 (a_2,b_2)	≈0		
17	8.33 (a_1,b_1)	≈0	−0.98 (a_1,b_2 / b_1,a_2)	S
	8.75 (a_2,b_2)	≈0		S

[a] The experimental IP's are from the following references: **1**, ref 7a; **3**, ref 7c; **4** and **5**, ref 7d; **6**, ref 7e; **7–9**, ref 7f; **11**. **13–17**, ref 7e. [b] The experimental EA's are from the following references: **1**, ref 19; **3–5**, ref 8; **1**, **2**, **6–17**, present study. [c] The STO-3G Koopmans' theorem splittings between the π_+ and π_- orbitals and between the π_+^* and π_-^* orbitals are given in parenthesis. [d] For **11** and **13** the first splitting is between the b_2 and a_2 orbitals and the second between the a_1 and b_1 orbitals (see Figure 11). For **12**, the first splitting is between the two a″ orbitals and the second between the a′ orbitals. [e] The "S" entry signifies that the splitting is small and not extractable from the ET spectra. [f] The two anion states reported for these compounds were resolved only when the spectra were obtained under low-retarding conditions.

σ, σ*, π, and π* orbitals; i.e., TB interactions are ignored in the zeroth-order picture. It is further assumed that one need only consider the two highest lying σ MO's and two lowest lying σ* MO's of the correct symmetry to mix with the various π orbitals.

The symmetries and coefficients of the σ-type MO's may be obtained from the "C" approximation[20] in which the Hückel model is used to determine the linear combinations of the sp^3 hybrid C–C σ orbitals (the C–H bonds are neglected). The data are displayed in Figure 4 for $n = 2$–6. Note that at this level of approximation, the pairing theorem[21] holds and that the MO's alternate in symmetry within each system of bonds. It also follows from the pairing theorem that the sequence of σ MO symmetries depends only on the parity of the number, n, of σ bonds, being σ_- above σ_+ for all even values of n (Figure 4a) and σ_+ above σ_- for all odd values of n (Figure 4b).[9]

Through-bond interactions now arise through mixing of these σ MO's with the symmetry-adapted combinations of the π basis

(19) Jordan, K. D.; Michejda, J. A.; Burrow, P. D. *Chem. Phys. Lett.* **1976**, *42*, 227.

(20) Sandorfy, C.; Daudel, R. *C. R. Acad. Sci.* **1954**, *238*, 93.

(21) Coulson, C. A.; O'Leary, B.; Mallion, R. B. *Hückel Theory for Organic Chemists*; Academic Press: New York, 1978; pp 88–110.

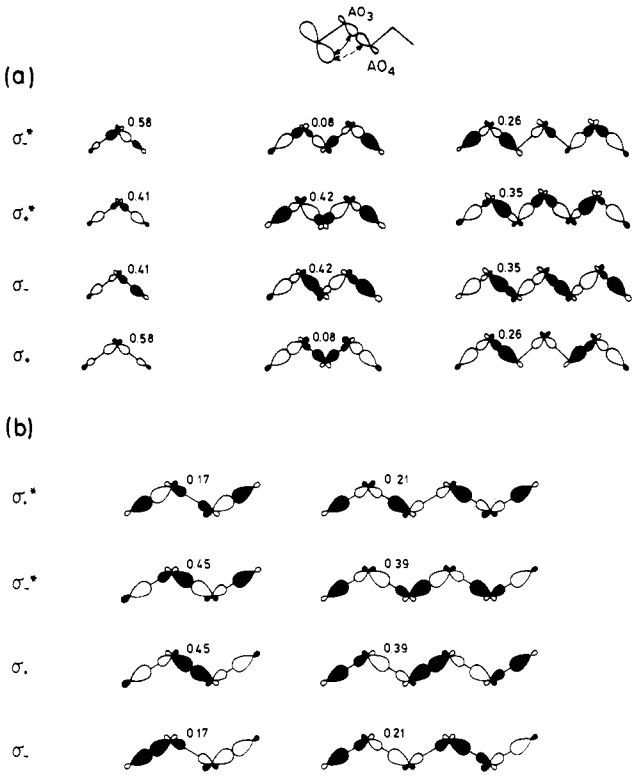

Figure 4. σ orbitals for chains containing (a) two, four, and six CC σ bonds, and (b) three and five σ bonds, as obtained from the "C" approximation.

MO's, π_+ and π_-, as shown in Figure 5 for $n = 4$ bonds. In the compounds considered here, the σ MO's come in pairs of symmetry-adapted combinations, the lower energy member of each pair being the in-phase combination (the unprimed set, e.g., σ_+, shown on the right-hand side of Figure 5) and the higher energy member being the out-of-phase combination (the primed set, e.g., σ_+', shown on the left-hand side of Figure 5). These orderings are confirmed by ab initio MO calculations on model compounds using the STO-3G basis set. OIT-4-B involving the filled π MO's arise through mixing of π_+ and π_- with the unprimed set of the σ MO's. However, π_-,σ_-^* and π_+,σ_+^* mixing can be ignored on account of the large σ^*/π energy gaps ($\approx$21 eV) and because of the small magnitudes of the π,σ^* interaction matrix elements (to be discussed later). The π_+ and π_- levels are therefore both raised in energy, through their respective mixing with the lower lying σ_+ and σ_- levels, by amounts that can be estimated from second-order perturbation theory:

$$E_{\bar{\pi}_+} = \epsilon_{\pi_+} + |H_{\pi_+\sigma_+}|^2/(\epsilon_{\pi_+} - \epsilon_{\sigma_+}) \quad (1a)$$

and

$$E_{\bar{\pi}_-} = \epsilon_{\pi_-} + |H_{\pi_-\sigma_-}|^2/(\epsilon_{\pi_-} - \epsilon_{\sigma_-}) \quad (1b)$$

where $H_{\pi_+\sigma_+}$ and $H_{\pi_-\sigma_-}$ are the interaction matrix elements; ϵ_{π_+}, ϵ_{π_-}, ϵ_{σ_+}, and ϵ_{σ_-} are the energies of the zeroth-order, i.e., unmixed orbitals; and $\bar{\pi}_+$ and $\bar{\pi}_-$ are used to distinguish the π obitals after interaction with the σ chain from the "pure", unmixed π orbitals. Assuming for the moment that $|H_{\pi_+\sigma_+}| \approx |H_{\pi_-\sigma_-}|$ (in general this is a poor approximation) and that through-space interactions are negligible, then the ordering of the levels (after interaction) will simply reflect that of the σ orbitals. Therefore, for $n = 4$ (right-hand side of Figure 5), and, indeed, for all even values of n, the $\bar{\pi}_+$ ($=\pi_+ - b\sigma_+$) level should be lower than the $\bar{\pi}_-$ ($=\pi_- - a\sigma_-$) level. However this ordering is reversed for systems with odd values of n (i.e., $\bar{\pi}_+$ above $\bar{\pi}_-$) because now σ_+ lies above σ_- (Figure 4).

That π,σ^* mixing can be neglected receives support from the PE spectra of the dienes **2**, **3**, **6**, and **7** (Figure 3) which reveal that both $\bar{\pi}_+$ and $\bar{\pi}_-$ levels for each diene are indeed raised relative to that of a noninteracting π level, represented by ethylene. In contrast, mixing of the π^* MO's with both σ' and σ'^* orbitals must be considered because the ET spectrum of **3** shows one π^* anion state to be more stable than that of ethylene and the other to be less stable. Although the π/σ^* and π^*/σ energy gaps should be comparable, the interaction matrix elements are generally smaller for the former (vide infra). The second-order changes in the π_+^* and π_-^* levels are given by

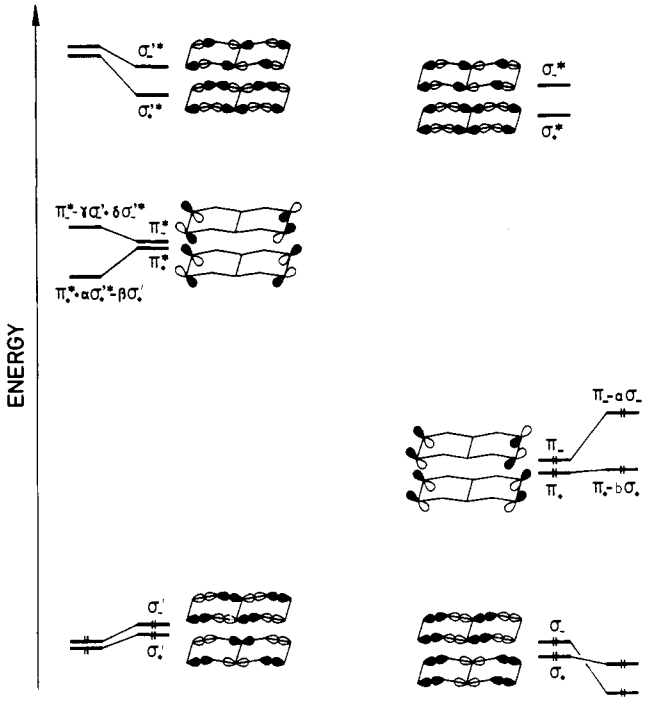

Figure 5. Interaction diagram depicting the through-4-bond interactions between the "pure" π_+, π_-, π_+^*, π_-^* orbitals and the σ and σ^* orbitals.

$$E_{\bar{\pi}_+^*} = \epsilon_{\pi_+^*} + |H_{\pi_+^*\sigma_+'^*}|^2/(\epsilon_{\pi_+^*} - \epsilon_{\sigma_+'^*}) + |H_{\pi_+^*\sigma_+}|^2/(\epsilon_{\pi_+^*} - \epsilon_{\sigma+'}) \quad (2a)$$

and

$$E_{\bar{\pi}_-^*} = \epsilon_{\pi_-^*} + |H_{\pi_-^*\sigma_-'^*}|^2/(\epsilon_{\pi_-^*} - \epsilon_{\sigma_-'^*}) + |H_{\pi_-^*\sigma_-}|^2/(\epsilon_{\pi_-^*} - \epsilon_{\sigma_-'}) \quad (2b)$$

Again assuming for simplicity that $|H_{\pi_+^*\sigma_+'^*}| \approx |H_{\pi_-^*\sigma_-'^*}| = A$ and $|H_{\pi_+^*\sigma_+'}| \approx |H_{\pi_-^*\sigma_-'}| = B$, one is led to the conclusion that the $\bar{\pi}_+^*$ orbital is more stable than the $\bar{\pi}_-^*$ orbital for even values of n intervening σ bonds as shown for $n = 4$ in the left-hand side of Figure 5. This follows from

$$E_{\bar{\pi}_+^*} - E_{\bar{\pi}_-^*} = A^2\left\{\frac{1}{\epsilon_{\pi_+^*} - \epsilon_{\sigma_+'^*}} - \frac{1}{\epsilon_{\pi_-^*} - \epsilon_{\sigma_-'^*}}\right\} + B^2\left\{\frac{1}{\epsilon_{\pi_+^*} - \epsilon_{\sigma_+'}} - \frac{1}{\epsilon_{\pi_-^*} - \epsilon_{\sigma_-'}}\right\} \quad (3)$$

in which both terms on the right-hand side are negative since the level sequences are σ_-' above σ_+' and $\sigma_-'^*$ above $\sigma_+'^*$.[22] However, because the level sequences are the reverse for odd values of n, i.e., σ_+' above σ_-' and $\sigma_+'^*$ above $\sigma_-'^*$, it follows that $\bar{\pi}_-^*$ lies below $\bar{\pi}_+^*$ for orbital interactions involving odd numbers of σ bonds.

The magnitude of the interaction matrix elements in eq 1 and 2 depends on the overlap of the π and π^* orbitals with the relevant σ and σ^* orbitals, which in turn can be reduced to the squares of the orbital coefficients. Estimates of these coefficients, obtained from the "C" approximation, are given in Figure 4.

The mixing between the σ and π orbitals occurs primarily through overlap of the π (or π^*) MO with that portion of the σ (or σ^*) MO which is contributed by the hybrid orbital on the carbon atom adjacent to the π bond, and designated as AO_3 in

(22) Note that $\epsilon_{\pi_+^*}$ and $\epsilon_{\pi_-^*}$ are degenerate since TS interactions between the localized π_A^* and π_B^* orbitals are negligible.

Figure 4. It can be seen that, for $n > 2$ σ bonds, the coefficient of AO_3 is larger in the highest occupied σ MO (i.e., σ_- for even values of n, and σ_+ for odd values of n) than in the second highest occupied σ MO (i.e., σ_+ for even n and $*_-$ for odd n). The most pronounced difference occurs for $n = 4$ bonds. From the pairing theorem, the coefficient of AO_3 is larger in the lowest vacant σ^* MO (σ_+^* for even n, σ_-^* for odd n) than in the second lowest vacant σ^* MO (σ_-^* for even n, σ_+^* for odd n). The trends in the σ' and σ'^* MO's are identical with those in the σ and σ^* MO's. Consequently, the interaction matrix elements vary in such a way as to reinforce the level orderings obtained from energetic considerations. If only the interactions of the π and π^* orbitals with the AO_3 hybrid orbitals were considered, the π/σ^* and π^*/σ mixing would be of comparable importance. However, mixing with the AO_4 hybrid orbitals (see Figure 4) is also significant, and (with the exception of the σ_- and σ_-^* orbitals of the 3-σ bond case) AO_3 and AO_4 are of the same phase in the σ orbitals and of opposite phase in the σ^* orbitals. As a result, the mixing of the π and π^* orbitals with the σ orbitals is enhanced (relative to what it would be if only interactions with AO_3 were important) and their mixing with the σ^* orbitals is reduced. This, combined with the large π/σ^* energy separations, makes π/σ^* mixing relatively unimportant. For the π^* orbitals, the combination of the differences in the energy denominators and the magnitudes of the interaction matrix elements with the σ and σ^* orbitals are such that the π^*/σ and π^*/σ^* interactions are comparable.

Whether the π_+^* and π_-^* orbitals of the dienes are stabilized or destabilized with respect to the π^* orbital of ethylene depends on whether the interaction is stronger with the occupied or unoccupied σ orbitals. The ET measurements show that one anion state of **3** is stabilized and the other destabilized with respect to that of ethylene.[8] Consideration of the relative magnitudes of the orbital coefficients and relative energies of the zeroth-order states leads to the conclusion that the π_+^* orbital is stabilized and that the π_-^* orbital is destabilized in this compound and also in 6-σ bond compounds such as **7**. Hence, π_+^* mixes more strongly with $\sigma_+'^*$ than with σ_+', whereas π_-^* mixes more strongly with σ_-' than with $\sigma_-'^*$.

In the monoenes the "+" and "−" symmetries are lost and the π orbital mixes with both the two highest occupied σ orbitals. (Mixing with the two lowest unoccupied σ^* orbitals is unimportant.) Also the π^* orbital mixes with the two highest occupied σ' and the two lowest unoccupied σ'^* orbitals, with the latter being greater for energetic reasons.

The above picture explains several experimental trends. Consider, for example, the interaction of the normalized $\pi_+ = 1/\sqrt{2}(\pi_A + \pi_B)$ and $\pi_- = 1/\sqrt{2}(\pi_A - \pi_B)$) orbitals with σ_+ and σ_-, respectively. Let the π_+ and π_- levels be raised by amounts $2x$ and $2y$, respectively, where

$$2x = |\langle \pi_+|H|\sigma_+\rangle|^2/(\epsilon_{\pi_+} - \epsilon_{\sigma_+}) \tag{4a}$$

and

$$2y = |\langle \pi_-|H|\sigma_-\rangle|^2/(\epsilon_{\pi_-} - \epsilon_{\sigma_-}) \tag{4b}$$

from which:

$$x = \frac{|\langle \pi_A|H|\sigma_+\rangle|^2}{\epsilon_{\pi_+} - \epsilon_{\sigma_+}} \text{ and } y = \frac{|\langle \pi_A|H|\sigma_-\rangle|^2}{\epsilon_{\pi_-} - \epsilon_{\sigma_-}}$$

From comparison of the π IP of ethylene with the π IP's of **3** one finds that $2x = -1.16$ eV and $2y = -2.03$ eV.[23] For the corresponding monoene, **19**, the π MO, which may be taken to be equivalent to π_A, is raised through mixing with σ_+ and σ_-, by an amount, $\Delta = x + y$, that is:

$$\Delta = \frac{|\langle \pi_A|H|\sigma_+\rangle|^2}{\epsilon_{\pi_+} - \epsilon_{\sigma_+}} + \frac{|\langle \pi_A|H|\sigma_-\rangle|^2}{\epsilon_{\pi_-} - \epsilon_{\sigma_-}} = x + y$$

(23) These values also contain a contribution from the inductive effect of the hydrocarbon framework which is present in **3** but absent in the ethylene reference molecule.

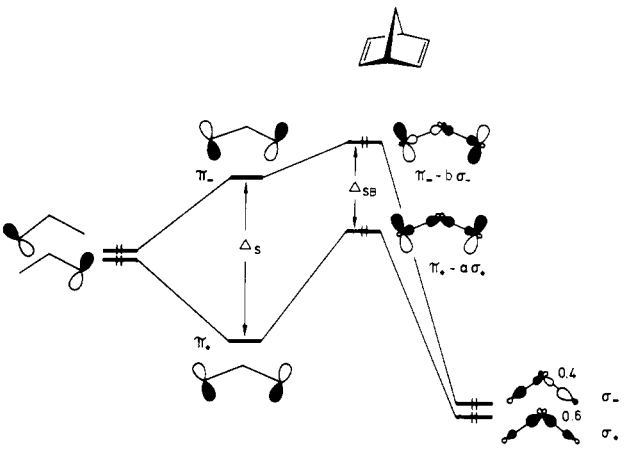

Figure 6. Correlation diagram depicting schematically the TP and TS interactions between the π and between the π^* orbitals of norbornadiene.

(The "+" and "−" symbols now refer to pseudosymmetries in the monoene.) This predicted value (−1.60 eV) is in excellent accord with the observation that the IP of **19** is 1.66 eV smaller than that of ethylene.

If the shifts in the π_+^* and π_-^* levels of **3** are denoted by $2z$ and $2w$, respectively, comparison of the EA's of **3** with that of ethylene gives $2z = 0.54$ eV and $2w = -0.28$ eV. This leads to the prediction that the EA of **19** should be shifted (relative to that of ethylene) by $z + w = 0.13$ eV, which is identical with the value determined experimentally.

Since the π^* orbitals mix with the σ' and σ'^* orbitals, we should actually write

$$w = w_{\sigma_+'} + w_{\sigma_+'^*}$$

and

$$z = z_{\sigma_-'} + z_{\sigma_-'^*}$$

However, it is not possible to determine the magnitudes of the individual contributions to w and z.

Although the compounds **1**, **3**, **6**, and **7** have been emphasized, the above model is applicable to **4**, **5**, and **8**–**10**. For **5** it is also necessary to allow for the TS interaction, particularly for the π^* orbitals. For compounds in which laticyclic hyperconjugation is possible (as in **4**, **8**, and **10**) one must allow for interaction of the π orbitals with both the C–C σ and CH_2 bridging groups.

In 2-σ bond systems, such as norbornadiene **1**, TS interactions are important and, unlike the 4-σ and 6-σ bond cases, the AO_3 orbital has a larger coefficient in the σ_+ and σ_+' orbitals than in the σ_- and σ_-' orbitals. Because the π_+/σ_+ and π_-/δ_- energy gaps should be similar, this implies that the TS interactions and OIT-2-B oppose one another. This is shown schematically for norbornadiene in Figure 6. The interactions between the occupied π orbitals are discussed first. The TS interactions result in a split of Δ_S. However, because the square of the coefficient AO_3 in σ_+ is about 2.1 times that in σ_-, it follows that TB interactions involving π_+ with σ_+ should be approximatley 2.1 times as large as those involving π_- with σ_- (assuming that after the TS interaction the π_+/σ_+ and π_-/σ_- energy gaps are similar). Thus the resulting splitting, ΔIP, due to both TS and OIT-2-B, is less than Δ_S. This simple model receives support from SPINDO SCF calculations,[24] which indicate that in norbornadiene the π_+/σ_+ TB interactions are approximately 2.5 times greater than the π_-/σ_- TB interactions.

In norbornadiene (and barrelene[25]) the TB destabilization of π_+ relative to π_- is not sufficiently great to invert the orbitals from their TS ordering, that is, π_+ below π_-. Interestingly, in triptycene TB interactions appear to destabilize the π_+ and π_- orbitals more equally, with the net result that the splitting between the π orbitals

(24) Heilbronner, E.; Schmelzer, A. *Helv. Chim. Acta* **1975**, *58*, 936.
(25) Haselbach, E.; Heilbronner, E.; Schroder, G. *Helv. Chim. Acta* **1971**, *54*, 154.

is determined largely by the TS interactions.[26]

As for the 4-σ and 6-σ bond systems, OIT-2-B with the σ'* and σ' orbitals shift the π* orbitals in opposite directions. In the 2-σ bond case the π_+* orbital should be destabilized and the π_-* orbital slightly stabilized, decreasing the splitting derived from the TS interaction. However, the net effect of the TB interactions with the σ' and σ'* orbitals appears to be quite small, and the splittings between the π_+* and π_-* orbitals of norbornadiene (and triptycene[27]) are due largely to the through-space interaction.

The above discussion has focused on molecules in which the ethylene groups are separated by an even number of σ bonds. In the case of an odd number of σ bonds, as in **2** and **6**, the σ and σ* orbitals (as well as their primed counterparts) have the opposite ordering (i.e., σ_- below σ_+ and σ_-* below σ_+*) than for the even-length chains. This in turn causes the ordering of the π and the π* orbitals to be reversed from the normal (i.e., TS) sequence. Earlier PES and theoretical studies have confirmed the π_- below π_+ ordering of the filled orbitals in **2**[7b] and **6**.[7e]

In the previous section it was noted that even though the low-retarding spectrum of **6** shows the two anion states to be split by 0.6 eV, the high-retarding spectrum shows only a single broad peak. Even allowing for the peak widths, one might expect that two features whose "midpoints" are separated by 0.6 eV should be resolved in thei high-retarding spectrum, especially since the high-retarding spectrum of **3** clearly resolves the two anion states which are split by 0.8 eV. That this is not possible in **6** is probably due to the fact that the cross section (i.e., intensity) of the second anion state is appreciably less than that of the first.

The scattering cross section is proportional to $[l(l+1)/E]\sin(\delta_l(E))$, where E is the incident electron energy, l the angular momentum associated with the orbital involved in the electron capture, and δ_l the phase shift. To determine which values of l are involved, one must make partial-wave expansions of the orbitals of interest. For atoms, the empty orbitals can be characterized by a single l value (i.e., s, p, d, etc.). However, for molecules an infinite number of l values are involved. If the symmetry is sufficiently high, a single l value often dominates. In **3**, **6**, and **7** the leading and presumably dominant values of l are $l = 1$ in the lower π* anion state and $l = 2$ in the excited π* anion state. Considering only the energy and symmetry differences, the second anion states of these compounds would thus be expected to be more pronounced than the first anion states. That this is not observed in practice may be due to the acceptance angle characteristics of the electron transmission instrument, which tend to make the higher lying resonances less pronounced than the lower lying resonances in the ET spectrum.

In the case of **2**, for which only one low-energy peak is seen in the ET spectrum, both anion states are characterized by $l = 1$, which should cause the second anion state to be broader and less pronounced than that in **3**, **6**, and **7**. However, this would not explain why the second anion state is not observed in **2** but is observed in the corresponding benzene analogue, **12** (vide infra).

C. Comparison with the Predictions of STO-3G Calculations. SCF calculations with the STO-3G basis set were carried out on the ground state of several of the molecules studied here. Geometries for **1**, **3–6**, and **11** were fully optimized at the HF/STO-3G level. Those for **7–9** were obtained from molecular mechanics calculations. Within the context of Koopmans' theorem,[6] the negatives of the energies of the filled and unfilled orbitals may be associated with the IP's and EA's, respectively. These estimates are crude as a result of the neglect of relaxation and correlation contributions to the ionization and electron attachment processes and the use of an inflexible basis set. Moreover, for unstable anions (that is, those lying energetically above the ground state of the neutral molecule), the variational principle is not applicable. Finally, errors in the geometries could introduce small ($\approx$0.1 eV) errors in the IP's and EA's. The calculated and experimental values of the splittings are reported in Table II. In view of the limitations mentioned above, the agreement between the two sets of splittings (for both the anion and the cation states) is remarkable. In all cases, including **5**, for which long-range TS interactions are important,[28] the calculated and experimental splittings (both π_+*/π_-* and π_+/π_-) agree to within 0.25 eV. Thus relaxation and correlation corrections are relatively unimportant for determining the magnitudes of the splittings resulting from TB interactions between the remote unsaturated groups.

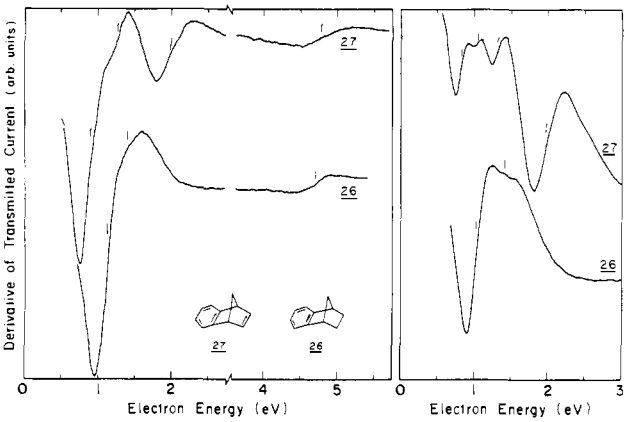

Figure 7. Derivative of the transmitted current as a function of electron energy in **26** and **27**. The spectra shown on the left were obtained under high-retarding conditions, while those on the right were obtained under low-retarding conditions.

The STO-3G splittings (ΔEA's and ΔIP's) of **3** and **7** agree to within 0.05 eV of the corresponding experimental values for these compounds. For **4** the STO-3G calculations give ΔIP = 0.52 eV, 0.08 eV larger than the experimental value and ΔEA = 0.54 eV, 0.22 eV smaller than experiment. Again, it is likely that long-range TS interactions, not accounted for with the STO-3G basis set, are responsible for this discrepancy in the splitting between the anion states of **4**. Evidence for this is provided by SCF calculations on a system comprised of two ethylene molecules, having the same orientation as the ethylenic groups in **4**. With the 3-21G basis set these calculations give a ΔEA value of 0.22 eV, whereas the STO-3G basis set, which does not contain diffuse functions, gives a value three times smaller. The somewhat larger errors in the STO-3G predictions for the splittings within the anion and the cation states of **6** may be due to the inadequacy of the STO-3G basis set for describing the cyclobutane portion of the molecule.

IV. Benzene Compounds

Before examining the ET spectra of the dibenzene compounds, it is instructive to consider first those of **26** and **27** which are shown in Figure 7. The ET spectrum of **26** displays structure due to anion formation at 1.12 and 4.70 eV. There is also a very weak shoulder near 1.4 eV, barely discernible in the high-retarding spectrum but more visible in the low-retarding spectrum. The energies of the two anion states of **26** are nearly the same as those of benzene (1.15 eV ($^2E_{2u}$) and 4.8 eV ($^2B_{2t}$)), the main difference being that the $^2E_{2u}$ ground state anion of benzene has very pronounced vibrational structure due to the excitation of the ring breathing mode.[4,12] It has been found that, in general, alkyl substitution causes a significant loss of visibility of vibrational structure in anion states, and it has been suggested that this is due to the symmetry lowering caused by the substitution.[12] Not surprisingly, the ET spectrum of **26** is nearly identical (including the weak feature at 1.4 eV) with that of *o*-xylene. Since both ESR measurements[29] and MO calculations[30] indicate that the two anion

(26) Haselbach, E.; Neuhaus, L.; Johnson, R. P.; Houk, K. N.; Paddon-Row, M. N. *Helv. Chim. Acta* **1982**, *65*, 1743.
(27) Balaji, V.; Jordan, K. D. *Chem. Phys. Lett.* **1985**, *119*, 294.

(28) (a) That TS interactions in **5** are indeed dominant is readily confirmed from the STO-3G calculated π*/π* splitting energy of 1.2 eV for two ethylene molecules placed in a geometry identical with that expected (see ref 28b) for the two double bonds in **5**. (b) Prinzbach, H.; Sedelmeier, G.; Kruger, K.; Goddard, R.; Martin, H.-D.; Gleiter, R. *Angew. Chem., Int. Ed. Engl.* **1978**, *17*, 271.
(29) Bolton, J. R. *J. Chem. Phys.* **1964**, *41*, 2455.

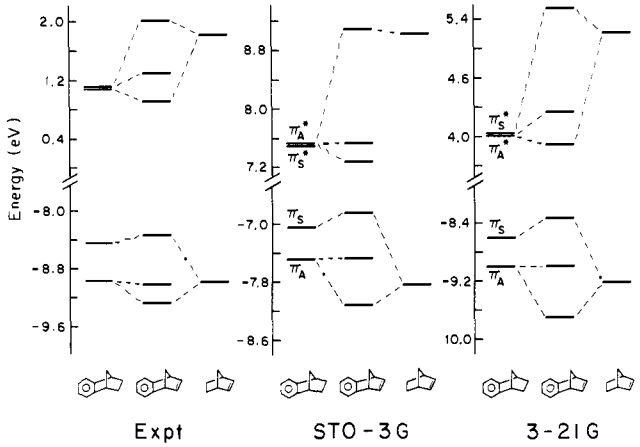

Figure 8. Correlation diagram comparing the negatives of the experimental and theoretical IP's and EA's of **26**, **27**, and norbornene (**18**). The theoretical IP's and EA's were obtained using both the STO-3G and 3-21G basis sets together with the Koopmans' theorem approximation.

states of *o*-xylene derived from the $^2E_{2u}$ state of the benzene anion are nearly degenerate (i.e., separated by less than 0.05 eV), it has been suggested that the "extra" 1.4-eV feature is due to a vibronic, pseudo-Jahn–Teller coupling between the two closely spaced states.[12] The similarity of the spectra of *o*-xylene and **26** leads us to suggest that the weak 1.4-eV feature of the latter is likewise due to vibronic interaction.

The spectra of several of the other benzene compounds considered here also display weak structure a few tenths of an eV above the first peak, leaving one faced with the task of deciding whether the weak feature should be identified with the second anion state or rather with vibronic structure resulting from the interaction of two nearly degenerate states. Although calculations can prove valuable in dealing with this problem, they were feasible only for the smaller molecules.

Under high retarding conditions the ET spectrum of **27** displays peaks at 0.92, 1.28, 2.01, and 4.78 eV. The low-retarding spectrum reveals that the 0.92-eV feature actually consists of a main peak at 0.82 eV and an additional feature, presumably due to vibrational excitation, at 1.04 eV. The 1.28-eV feature is sharper (and displaced to 1.34 eV) in the low-retarding spectrum. In order to determine whether the 1.28-eV feature is due to vertical attachment to the second anion state or due to the vibronic interaction between two nearly degenerate anion states, ab initio calculations were performed with both the STO-3G minimal and 3-21G split-valence[31] basis sets. Assuming the validity of Koopmans' theorem, the IP's and EA's were equated with the negatives of the energies of the filled and unfilled orbitals of the neutral molecule. These calculations indicate a sizable splitting (0.30 and 0.45 eV using the STO-3G and 3-21G basis sets, respectively) between the first two anion states, leading us to conclude that the 1.28-eV feature indeed corresponds to the excited anion state.

The mixing of the benzene π_A* orbital with the ethylenic π* orbital gives rise to the 0.92- and 2.01-eV anion states, whereas the 1.28-eV anion state derives from the π_S* component of the benzene e_{2u} π* orbital. As for norbornadiene and **11** (to be considered below), TB and TS interactions counteract each other in both the cation and anion states of **27**, resulting in net splittings less than those expected were only TS interactions operative.

The EA's and IP's of *o*-xylene, **18**, **26**, and **27** are summarized in the correlation diagram given in Figure 8. This correlation diagram reveals a major weakness of the STO-3G and 3-21G calculations for the "mixed" ethylene–benzene compounds, namely

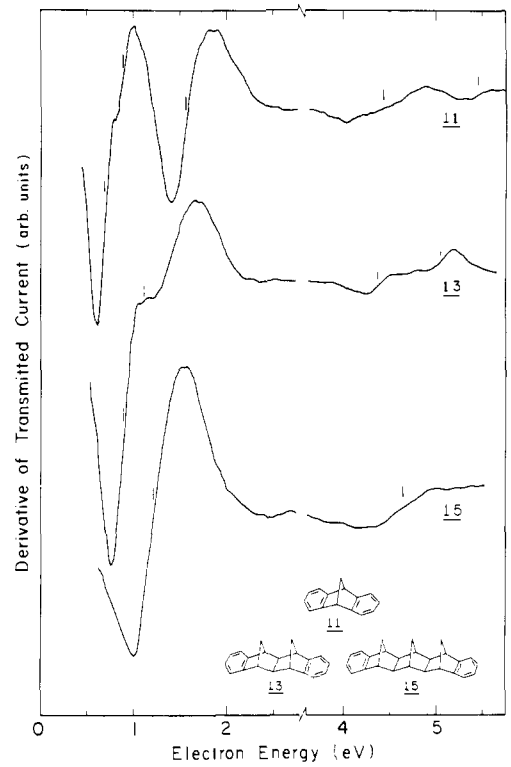

Figure 9. Derivative of the transmitted current as a function of electron energy in **11**, **13**, and **15**. The two features indicated by the dashed vertical lines in the ET spectrum of **13** are believed to be due to an impurity of a monobenzene compound.

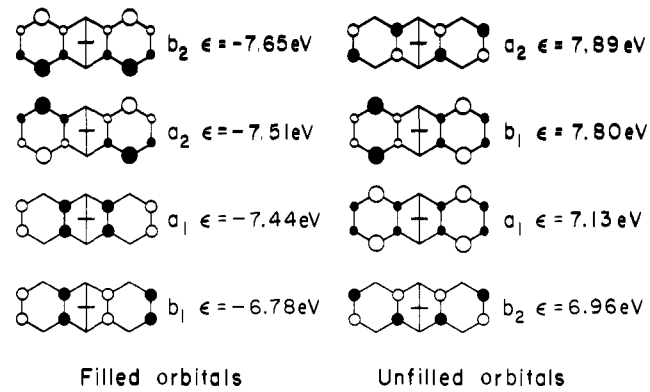

Figure 10. π and π* MO's of dibenzonorbornadiene derived from the e_{1g} (π) and e_{2u} (π*) orbitals of benzene. The MO symmetries and coefficients are from STO-3G calculations.

that they do not give good values for the relative IP's or EA's of the noninteracting ethylene and benzene moieties. As a result, there are significant errors in the calculated splittings for the anion and cation states of **27**.

The ET spectra of **11**, **13**, and **15** are compared in Figure 9. The ET spectrum of compound **11** has structure at 0.67, 0.88, 1.55, 4.45, and 5.45 eV. In addition the 1.55-eV feature has a weak shoulder near 1.65 eV. We believe that the 0.67-, 0.88-, 1.55-, and 1.65-eV features are due to the four anion states derived from the e_{2u} orbitals of the benzene entities. Support for this assignment is provided by STO-3G calculations, which give a splitting of 0.17 eV between the first pair (b_1 and a_1) of empty π* orbitals and 0.09 eV between the second pair (b_2 and a_2). The features at 4.45 and 5.45 eV should originate from the 4.8-eV anion state of benzene.

Figure 10 gives the symmetries and relative sizes of the coefficients of the first four unoccupied π* and highest four occupied π orbitals of **11**. (In this figure the mixing with the orbitals of the σ frame has been neglected.) The $^2B_2$ and $^2A_2$ anion states of **11** are derived from the π_A* component of the e_{2u} π* orbital

(30) 3-21G calculations give a Koopmans' splitting of only 0.03 eV between the two anion states.
(31) Binkley, J. S.; Pople, J. A.; Hehre, W. J. *J. Am. Chem. Soc.* **1980**, *102*, 939.
(32) Minz, D. M.; Kupperman, A. *J. Chem. Phys.* **1979**, *71*, 3499.
(33) Rabalais, J. W. *Principles of Ultraviolet Photoelectron Spectroscopy*; Wiley-Interscience: New York 1977.

of benzene and the $^2A_1$ and $^2B_1$ anion states from the π_S^* component. The first pair of anion states ($^2B_2$ and $^2A_1$) represent the bonding and the second pair ($^2A_2$ and $^2B_1$) the antibonding combinations of the localized benzene orbitals. As expected from the magnitudes of the coefficients of the π^* orbitals and the dominance of through-space interactions, the relative energies of the states are predicted to be $^2B_2$ below $^2A_1$ and $^2B_1$ below $^2A_2$. Both STO-3G calculations and ET measurements give a B_2/A_2 splitting 1.4 times the A_1/B_1 splitting, much less than the 3.0 value expected from the ratio of the squares of the coefficients of the relevant MO's of benzene. This is due largely to the presence of additional through-space interactions between the diagonal pairs of atoms, i.e., C_{4a},C_{8a} and C_{9a},C_{10a} in **11**. Such interactions would increase the (a_1,b_1) splitting but decrease the (b_2,a_2) splitting.[27]

The ET spectrum of compound **13** displays pronounced peaks at 0.90, 1.43, 4.40, 4.72, and 5.08 eV as well as a very weak feature at 1.15 eV. In **13**, unlike **11**, through-space interactions are negligible, and the observed splittings arise almost entirely from through-bond interactions. The four anion states derived from the $^2E_{2u}$ anion of benzene almost certainly lie in the 0.9–1.4 eV region. This seems to suggest that the $^2A_1$ and $^2B_2$ states both fall near 0.9 eV and that the $^2A_2$ and $^2B_1$ states both fall near 1.43 eV. This is supported by STO-3G calculations which yield splittings of 0.02 and 0.10 eV for the A_1/B_2 and A_2/B_1 pairs of anion states, respectively. The weak features near 1.15 and 4.72 eV probably arise from an impurity of a monobenzene compound.

Since the coefficients of the a_2 and b_2 π^* orbitals are larger at the sites of overlap with the σ framework than those of the a_1 and b_1 π^* orbitals, the near degeneracy between the $^2A_1$ and $^2B_2$ and between the $^2A_2$ and $^2B_1$ pairs of anion states is at first surprising. However, this is entirely consistent with the relative energies of the σ and σ^* orbitals with which the π^* orbitals mix. In particular, it should be noted that the b_2 and a_2 π^* orbitals mix with the σ' and σ'^* orbitals, while the a_1 and b_1 orbitals mix with the σ and σ^* orbitals (see, for example, Figure 5). The σ orbitals are more stable than the corresponding σ' orbitals (i.e., σ_+ lies below σ_+' and σ_- below σ_-'), and the σ^* orbitals are more stable than the corresponding σ'^* orbitals.

As noted previously, the splitting between the A_1 and B_1 cation states of **13** is only 1.4 times smaller than the splitting between the corresponding cation states of **3**. Since the 0.9- and 1.4-eV features in the ET spectra each consist of overlapping anion states, it is difficult to get precise energies to determine the ratios of the splittings of the anion states of **3** and **13**. STO-3G calculations give a splitting of 0.37 eV between the A_1 and B_1 anion states of **13** as compared to 0.81 eV for **3**.

The 4.4- and 5.1-eV features in the ET spectrum are tentatively assigned to the two anion states derived from the benzene b_{1g} π^* orbital (having b_2 and a_2 symmetry, respectively). The 0.7-eV splitting between these two states is 1.4 times that in the lower lying B_2 and A_2 anion states, consistent with the squares of the coefficients of the relevant π^* orbitals $[(0.50/0.41)^2]$.

The ET spectrum of compound **15** displays peaks at 1.25 and 4.75 eV. Apparently in this compound the four anion states derived from the benzene e_{2u} π^* orbitals are very close in energy and comprise the peak at 1.25 eV. The two anion states derived from the benzene b_{1g} π^* orbital give rise to the peak at 4.75 eV. The width ($\approx$0.5 eV) of the 1.25-eV feature suggests that there is a small (0.1–0.2 eV) splitting between these four anion states in this energy range.

A correlation diagram summarizing the IP's and EA's of **11**, **13**, **15–17**, **26**, *o*-xylene, and benzene is given in Figure 11. The main reason for the rather different appearance of the correlation diagrams for the π than for the π^* levels is that there is an appreciable splitting between the π_S and π_A orbitals of **26**, and *o*-xylene, whereas the π_S^* and π_S^* orbitals of these molecules remain nearly degenerate. This is the result of hyperconjugative interactions which are much more important for the π_S than for the π_A orbital and are relatively unimportant for the π_S^* and π_A^* orbitals. The large splitting between the b_1 and a_1 π orbitals of **16** derives almost entirely from laticyclic hyperconjugation, which is not possible for the corresponding π^* orbitals.

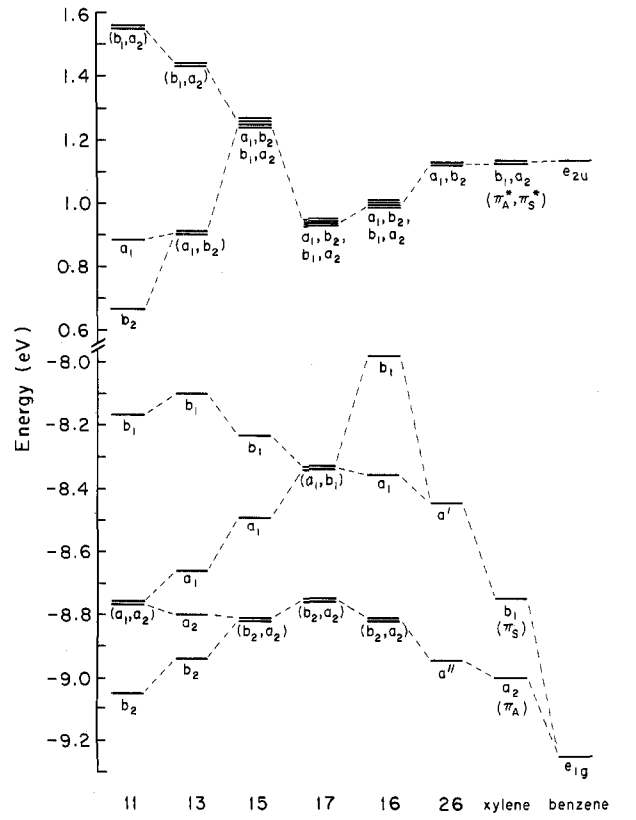

Figure 11. Correlation diagram giving the experimental IP's and EA's of **11**, **13**, **15–17**, **26**, *o*-xylene, and benzene.

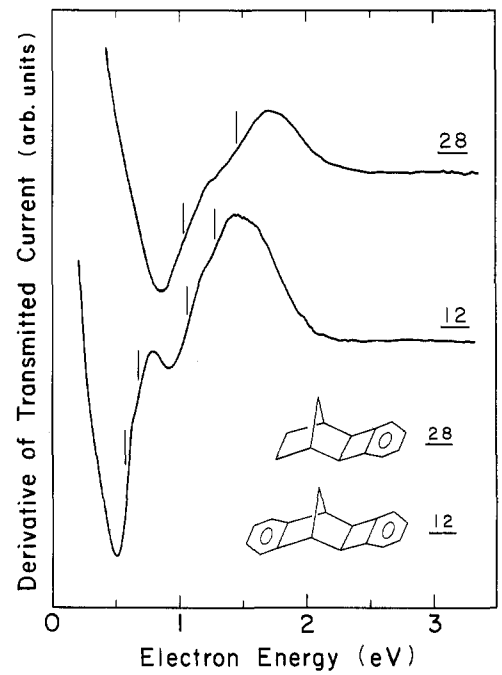

Figure 12. Derivative of the transmitted current as a function of the electron energy in **12** and **28**.

The ET spectrum of **12** and **28** are given in Figure 12, and the spectra of **14**, **16**, and **17** are reproduced in Figure 13. The ET spectrum of **28** has a pronounced feature at 1.05 eV with a shoulder at 1.45 eV. The splitting between these two features and their combined width are both greater (by 0.1 and 0.2 eV, respectively) than the corresponding values for **26**. This suggests that the appearance of two features in the 1-eV region of the ET spectrum of **28** may be due to a true splitting between the two anion states rather than to vibronic coupling between two nearly degenerate states. Support for this possibility is provided by the

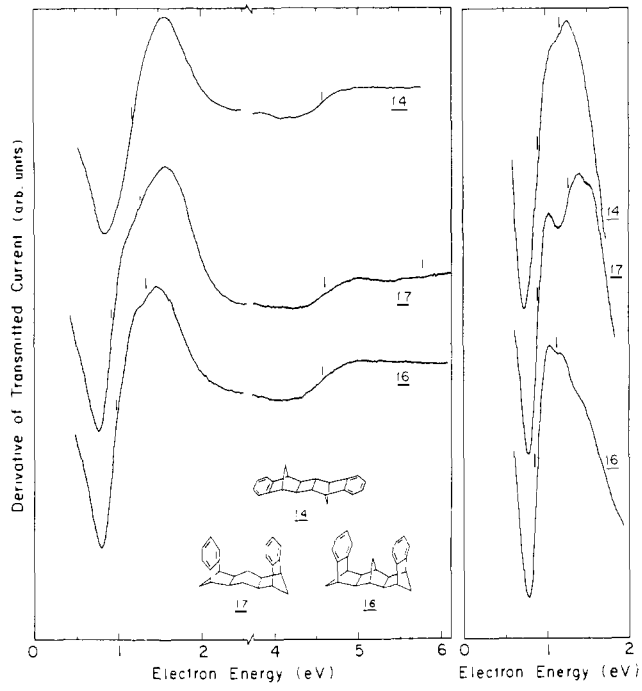

Figure 13. Derivative of the transmitted current as a function of electron energy in **14**, **16**, and **17**. The spectra on the left of the figure are obtained under high-retarding conditions and those on the right under low-retarding conditions.

results of calculations on benzene fused with a cyclobutane ring. For this system the Koopmans' theorem splitting between the a_2 and b_1 π^* MO's (derived from the benzene e_{2u} π^* MO) is 0.26 and 0.36 eV with the STO-3G and 3-21G basis sets, respectively.

Compound **12**, in which the two benzene rings are separated by three σ bonds, displays peaks at 0.59, 0.68, 1.07, 1.29, 4.46, and 5.5 eV. The four features below 1.3 eV are attributed to the four anion states derived from the interaction of the benzene e_{2u} π^* orbitals. Specifically, we attribute the first two features to electron capture into the π_-^* orbitals and the second pair to electron capture into the π_+^* orbitals. The π_-^* below π_+^* ordering is that expected for OIT-3-B interactions. This assignment is confirmed by STO-3G calculations which also indicate that the first and third anion states are of a'' symmetry (i.e., derive from the minus and plus combinations, respectively, of the π_A^* orbitals) and the second and fourth anion states are of a' symmetry (and derive from the minus and plus combinations of the π_S^* orbitals of the benzenes). The two states near 4.5 and 5.5 eV are likewise attributed to the anions derived from the b_{1g} π^* orbitals of the benzene rings.

Compound **14**, in which the two benzene rings are separated by five σ bonds, displays peaks at 1.19 and 4.55 eV in its high-retarding ET spectrum. The 1.19-eV feature has a width of 0.7 eV, suggesting that there is a small splitting between the four anion states derived from the benzene e_{2u} π^* orbitals. Under low-retarding conditions the first peak is found to consist of a large peak at 0.92 eV with a weak shoulder at 1.17 eV. It is not known whether this shoulder is due to a splitting between the anion states, vibrational structure, or a vibronic interaction between nearly degenerate anion states. The low-retarding ET spectrum of the corresponding diene **6** showed two peaks separated by 0.6 eV. This leads one to expect a splitting between the A_u/B_g pair of anion states of **14** of the order of 0.3 eV, which is certainly consistent with the splitting observed in the low-retarding spectrum.

Compounds **16** and **17**, which differ only by the presence of the bridging methylene group in the former, give very similar ET spectra. The high-retarding spectrum of the latter moleucle gives peaks at 0.93, 1.28, and 4.68 eV, and the former molecule at 0.98, 1.33, and 4.55 eV. The low-retarding spectra are even more structured, with that of **17** having pronounced peaks at 0.90 and 1.27 eV and weaker features at 1.5 and 1.1 eV. The low-retarding spectrum of **16** has its main feature at 0.90 eV and a series of weaker features at 1.1, 1.3, and 1.5 eV. Since the ET spectra of the corresponding dienes, **8** and **9**, did not display splittings between the anion states, and since the splitting in the anion states of **16** and **17** should be smaller than in the dienes, it is not expected that any of the additional features at low energy arise from splittings between the electronic states. Rather it is believed that the feature near 1.3 eV (which is especially pronounced in **17**) is of pseudo-Jahn–Teller origin and that the weaker structure is due to vibrational excitation of the ring. It is not known why the vibrational structure is more visible in these two compounds than in the other benzene compounds studied.

Although the a_2 and b_2 π^* orbitals of **16**, derived from the antisymmetric components of the e_{2u} π^* benzene orbitals, are prevented by symmetry from laticyclic conjugation, such interaction is possible in the a_1 and b_1 π^* orbitals derived from the symmetric component. However, owing to the small values of the coefficients of the π_s^* component of the e_{2u} π^* orbital at the positions of fusion of the bridging benzene rings, such interactions are expected to be too small to be observed.

V. Distance Dependence of Through-Bond Interactions

The π-ΔIP and π^*-ΔEA values for the diene **7** are impressively large and provide the first unequivocal experimental evidence that OIT-n-B of this magnitude (ca. 0.3 eV) can operate over such large distances (7 Å direct[34] or 9 Å if traced through the connecting σ bonds). The decay of π-OIT-n-B along the series of all-trans dienes **2**, **3**, **6**, and **7** (n = 3–6), as measured by ΔIP, is approximately exponential[35] and is well represented by

$$\ln \Delta IP = -0.46n + 1.56 \quad (5)$$

From this equation, it can be seen that through-bond interactions involving π MO's of the dienes are very long-range indeed. For example, a through-bond splitting energy of ca. 0.003 eV is predited for values of n as large as 16 or, equivalently, for an inter-π-orbital separation of 21 Å! Although such a splitting is negligible from a spectroscopic (PES or ETS) point of view, is is sufficiently large to enhance dramatically the rates of electron-transfer processes, as will be discussed below. The ETS data for the dienes **3**, **6**, and **7** likewise indicate a weak dependence of π^*-OIT-n-B on n which is comparable to that found for π-OIT-n-B.

That through-bond interactions are so strong in both radical-cation and radical-anion states of the dienes is probably due to the structural features of the norbornene fragment in these systems. The STO-3G optimized geometry of norbornene[36] reveals that the π MO and the C–C σ MO's are in almost perfect alignment to maximize hyperconjugative interactions between them.

The PES and ETS data also indicate that benzene–benzene through-bond interactions involving the π_S and π_A^* MO's show only a weak distance dependence, similar to that found for the corresponding dienes. However, the magnitude of the through-bond interactions are weaker in the dibenzo series, relative to the corresponding dienes, because of the dependence of such interactions on the square of the appropriate coefficient in the MO of the chromophore. Furthermore, orbital interactions between the π HOMO's of the naphthalene rings in the naphthalene annulated analogues of the dienes **1–4** and **6–8**, in which the norbornyl framework is attached at positions 2 and 3 of the naphthalene rings, should be about seven times weaker than in the dienes because of the coefficient of the highest filled MO (π_A) of naphthalene is only 0.26 (compared to 0.7 for a double bond).

VI. Through-Bond Interactions and Intramolecular Electron Transfer

In this section, we show that the results of our PES and ETS studies on the dienes and dibenzo compounds, described herein,

(34) Paddon-Row, M. N.; Englehardt, L. M.; Skelton, B. W.; White, A. H.; Jorgensen, F. S.; Patney, H. K. *J. Chem. Soc., Perkin Trans. 2*, in press.
(35) Paddon-Row, M. N.; Cotsaris, E.; Patney, H. K. *Tetrahedron* **1986**, *42*, 1779.
(36) Rondan, N. G.; Paddon-Row, M. N.; Caramella, P.; Houk, K. N. *J. Am. Chem. Soc.* **1981**, *103*, 2436.

point to the possible involvement of through-bond orbital interactions in a variety of long-range intramolecular electron-transfer processes.

Single electron transfer plays a pivotal role in a variety of thermal[37] and photochemical[38] processes, the most spectacular of which occur in biological systems. A wealth of evidence has been gathered that shows that both thermal[37] and photoinduced[13,39-44] electron transfer between a donor and acceptor pair can occur over distances that are considerably greater than the sum of the donor and acceptor van der Waals radii. Indeed, many biological electron-transfer processes involve such long-range events. This is dramatically illustrated by the primary steps in photosynthesis[45] in which extremely rapid (subnanosecond) photoinduced electron transfer occurs along a gradient of redox centers which are rigidly embedded in a lipid membrane and separated from each other by well-defined distances of 10 Å or greater.[46]

Recent studies on a number of modified biological and nonbiological systems, containing redox centers at widely different distances, have revealed electron-transfer rates ranging from the picosecond regime to many seconds.[14,47-57] Miller and co-workers have provided some superb examples of rapid, long-range, thermal intramolecular electron transfer occurring over large distances.[14,57] Thus, the rate constant for intramolecular electron transfer from the biphenyl donor to the cinnamoyl acceptor in the anion radical of **32** was found to be greater than 10^9 s^{-1}, notwithstanding a donor–acceptor edge-to-edge distance of ca. 10 Å.

A central issue in electron-transfer dynamics is the question of the mechanism of long-range electron transfer in which the donor and acceptor groups are at least 6 Å apart, either as separate entities or connected to each other through a nonconjugated σ-bonded framework. Does it occur via direct electron tunnelling through space, or does it occur via a through-bond mechanism? Some sort of through-space electron tunneling has, until recently, been the favored mechanism, being proposed, for example, to account for the rapid rates of intramoleclar electron transfer observed in anion radicals such as **32**[14] (but which was subsequently rejected in favor of the through-bond mechanism).[57] The through-bond mechanism involves, as discussed at length above, coupling of the donor and acceptor π (or π^*) orbitals with the orbitals of the interconnecting σ-bond framework. Although this mechanism has been occasionally advocated,[2,42,57,58] it has not, until recently, enjoyed much popularity. This is largely on account of the widely held belief that coupling between σ and π orbitals is too weak to allow through-bond mediated electron transfer to occur.

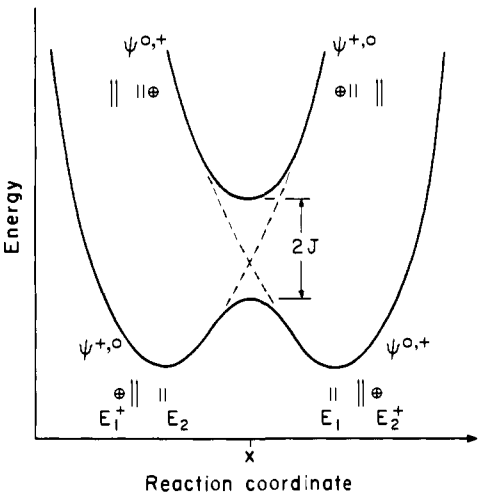

Figure 14. Schematic energy profiles for electron transfer between two ethene molecules, E_1 and E_2, in a cation-radical complex. The dashed lines represent the diabatic surfaces, and the solid lines the resulting adiabatic surfaces. The splitting of the adiabatic surfaces is equal to $2J$. The reaction coordinate mainly describes the changes in bond lengths that accompany electron transfer.

However, the results of our PE and ET spectral studies on the above dienes and dibenzo analogues clearly indicate that this belief is unjustified, and that through-bond interactions are energetically far from insignificant even for double bonds that are separated by distances as large as 7.5 Å, as in **7**. The following analysis shows that the PE and ET data are, indeed, relevant to the question of the importance of through-bond interactions to electron-transfer dynamics. Consider a gas-phase thermal electron-transfer process taking place between two identical ethylene groups of a cation radical complex, according to the equation:

$$E_1^+ + E_2 \rightleftarrows E_1 + E_2^+ \qquad (6)$$

where E_1^+ is the cation radical of ethylene 1 (configuration π_1) and E_2 is neutral ethylene 2 (configuration π_2).

The reaction coordinate diagram for this process is shown in Figure 14. The reaction coordinate represents the geometrical changes of the molecules accompanying electron transfer. For simplicity, these are merely indicated schematically by changes in the double-bond length, from a long, stretched bond in the cation radical to a short bond in the neutral species. The potential energy hypersurface may be analyzed in terms of two intersecting diabatic hypersurfaces, one representing the electronic configuration $\psi^{0,+} = \{E_1,E_2^+\}$ and the other by the configuration $\psi^{+,0} = \{E_1^+,E_2\}$. The intersection of the surfaces produces a seam along which the geometries of the two ethylene units are identical. The minimum energy point on this seam corresponds to X on the reaction coordinate (Figure 14), through which electron transfer is most likely to occur. Along the seam of intersection, the two configurations mix the most strongly, resulting in an avoided crossing of the surfaces. The magnitude of this avoided crossing is given by $2J$, where J is the electron coupling (transfer) integral, and depends on the interaction matrix element $\langle\psi^{+,0}|H_{el}|\psi^{0,+}\rangle$, where H_{el} is the electronic (Born–Oppenheimer) Hamiltonian for the system.

Thermal electron transfer can now be envisaged as taking place adiabatically on the lower surface of Figure 14, the rate constant k for which may be analyzed in terms of transition state formalism:[59-62]

$$k = (k_B T/h)k\tau \exp(-\Delta G^{\ddagger}/k_B T) \qquad (7)$$

(37) Miller, J. R.; Beitz, J. V.; Huddleston, R. K. *J. Am. Chem. Soc.* **1984**, *106*, 5057 and references cited therein.
(38) Creed, D.; Caldwell, R. A. *Photochem. Photobiol.* **1985**, *180*, 715.
(39) Warman, J. M.; de Haas, M. P.; Oevering, H.; Verhoeven, J. W.; Paddon-Row, M. N.; Oliver, A. M.; Hush, N. S. *Chem. Phys. Lett.* **1986**, *128*, 95..
(40) Kuhn, H. *J. Photochem.* **1979**, *10*, 111.
(41) Mobius, D. *Ber. Bunsenges. Phys. Chem.* **1978**, *82*, 848.
(42) Pasman, P.; Verhoeven, J. W.; de Boer, Th. J. *Chem. Phys. Lett.* **1978**, *59*, 381.
(43) Pasman, P.; Koper, N. W.; Verhoeven, J. W. *Recl. Trav. Chim. Pays-Bas* **1982**, *101*, 363.
(44) Li, T. T.-T.; Weaver, M. *J. Am. Chem. Soc.* **1984**, *106*, 6107.
(45) Jortner, J. *J. Am. Chem. Soc.* **1980**, *102*, 6676.
(46) Deisenhofer, J.; Epp, O.; Miki, K.; Huber, R.; Michel, H. *J. Mol. Biol.* **1984**, *180*, 385; *Nature (London)* **1985**, *318*, 618.
(47) Isied, S. S.; Worosila, G.; Atherton, S. *J. Am. Chem. Soc.* **1982**, *104*, 7659.
(48) McLendon, G. L.; Winkler, J. R.; Nocera, D. G.; Mauk, M. R.; Mauk, A. G.; Gray, H. B. *J. Am. Chem. Soc.* **1985**, *107*, 739.
(49) McGourty, J. L.; Blough, N. V.; Hoffman, B. M. *J. Am. Chem. Soc.* **1983**, *105*, 4470.
(50) Isied, S. S.; Kuehn, C.; Worosila, G. *J. Am. Chem. Soc.* **1984**, *107*, 1722.
(51) McLendon, G. L.; Miller, J. R. *J. Am. Chem. Soc.* **1985**, *107*, 7811.
(52) Isied, S. S.; Vassilian, A.; Magnuson, R. H.; Schwarz, H. A. *J. Am. Chem. Soc.* **1985**, *107*, 7432.
(53) Gust, D.; Moore, T. A. *J. Photochem.* **1985**, *29*, 173.
(54) Schmidt, J. A.; Siemiarczuk, A.; Weedon, A. C.; Bolton, J. R. *J. Am. Chem. Soc.* **1985**, *107*, 6112.
(55) Wasielewski, M. R.; Niemczyk, M. P.; Svec, W. A.; Pewitt, E. B. *J. Am. Chem. Soc.* **1985**, *107*, 5562.
(56) Joran, A. D.; Leland, B. A.; Geller, G. G.; Hopfield, J. J.; Dervan, P. B. *J. Am. Chem. Soc.* **1984**, *106*, 6090.
(57) Closs, G. L.; Calcaterra, L. T.; Green, N. J.; Penfield, K. W.; Miller, J. R. *J. Phys. Chem.* **1986**, *90*, 3673.
(58) Paddon-Row, M. N.; Patney, H. K.; Peel, J. B.; Willet, G. D. *J. Chem. Soc., Chem. Commun.* **1984**, 564.
(59) Marcus, R. A. *J. Chem. Phys.* **1956**, *24*, 966; **1965**, *43*, 679.

where $\Delta G^{\ddagger}$ is the free energy of activation, k_B is Boltzmann's constant, and k and τ are the electronic and nuclear transmission coefficients, respectively. The electronic transmission coefficient is a measure of the probability that the system remains on the lower adiabatic surface during electron transfer, and depends on the square of the electronic coupling integral,[62] i.e., J^2. The rate of electron transfer therefore also depends on the magnitude of J^2. In the high-temperature limit,[62] eq 7 can be recast as:

$$k = \frac{4\pi^2}{h} J^2 \left[\frac{1}{4\pi k_B T \chi} \right]^{1/2} \exp\left\{ -\frac{(\chi + E_0)^2}{4 k_B T \chi} \right\} \qquad (8)$$

Where χ is the vibronic coupling energy ("reorganization energy"), and E_0 is the overall energy change accompanying electron transfer ("driving force"). In the high-temperature limit, the Marcus rate constant k depends on the three variables J, χ, and E_0 (in addition to T, of course). Although χ and E_0 are important, it is the dependence of k on J that largely determines the distance dependence of the electron-transfer rate.[62]

The splitting π-ΔIP determined from the energy difference between the (Franck–Condon) vertical π-IP's for the formation of the π_+ and π_- cations provides a direct measure of $2J$ for the cation states of a particular diene. The nexus between π-ΔIP and J enables an estimate to be made of the effect of through-bond coupling on the distance dependence of J and, hence, of the rates of electron transfer within the ground state of the cation radicals of the nonbornylogous dienes **6** and **7** and higher homologues. Extrapolated values of J for cation radicals of higher homologues of **7** can be obtained from eq 5, although we emphasize the approximate nature of this equation. This leads to the conclusion that the electron coupling integral J shows a very weak distance dependence as a result of through-bond interactions being, for example, only 200 times smaller in the hypothetical 17-bond diene (r = 21 Å) than in the 5-bond diene **6** (r = 6.2 Å). Because of its dependence on J^2, the electron transfer rate displays a stronger distance dependence than does J itself, being attenulated by a factor of 10^5 by an increase in distance r from 6 to 21 Å. Nevertheless, impressively large rates of electron transfer are expected in cation radicals of norbornylogous dienes, even when the double bonds are separated by 17 σ bonds or, equivalently, by 21 Å! (We estimate that thermal electron transfer could be as fast as 2×10^8 s^{-1} in such a case.)[63]

The rates of electron transfer in the ground-state cation radicals of the dibenzo analogues, such as **12–15**, should be slower than those for the corresponding dienes, because the value of $2J$ (i.e., π-ΔIP) found for these compounds is about 1.2–1.6 times smaller than that found for the dienes (vide supra). Nevertheless, a substantial rate of electron transfer, of the order of 10^8 s^{-1}, is calculated for a 14-bond dibenzo norbornylogous compound (benzene–benzene separation of ca. 17 Å) and for a 12-bond dinaphtho analogue (naphthalene–naphthalene separation of ca. 15 Å).[63]

This analysis cannot strictly be applied to the ET data because the anionic states "probed" by this technique are actually unbound states for the isolated unsolvated molecules. In general, the energy separations between the low-lying anion states of gas-phase molecules and those of their solvated counterparts are quite close.[16] Hence, it is reasonable to assume that the ET data do prove a qualitative measure of the EA splitting that would obtain for the anion states of the solvated molecules.[64] Consequently, we predict from the ET data that TB coupling can also give rise to extremely rapid long-range thermal electron transfer within anion radicals.

The effect of pure through-space orbital interactions on the distance dependence of both J and electron-transfer rates in cation radicals of dienes has been estimated from the computed ΔE_π (=$2J$ via Koopmans' theorem) splitting energies for a model "diethylene" complex.[63] For the complex with the two ethylenes separated by 7.5 Å (corresponding to **7**), the electron transfer rate is predicted to be four orders of magnitude slower than that deduced from the through-bond model, while when the two ethylene molecules are separated by 21 Å, the TS transfer rate is about 10^{17} times smaller than the TB rate.[63]

These considerations lead us to conclude that electron transfer in cation and anion radicals of dienes **6** and **7** and higher homologues, in which the double bonds are separated by more than 6 Å, should take place almost exclusively via the through-bond mechanism, the through-space mediated process being insignificant in comparison.

Clearly, the above analysis, together with the PE and EA data for the dienes (**2**, **3**, **6**, and **7**) and the dibenzo systems (**12–15**) suggest more strongly that through-bond interactions, but not through-space interactions, can give rise to extremely rapid rates of electron transfer over large distances (i.e., >10 Å) in the cation-radical and anion-radical states of these and homologous compounds.

The extraordinarily rapid rates of photoinduced intramolecular electron transfer found for rigid compounds such as **31**, in which the two chromophores are separated by a varying number of norbornyl and bicyclo[2.2.0] units, certainly point to the involvement of through-bond interactions in these processes.

VII. Conclusions

Electron transmission spectroscopy has been utilized to determine the vertical electron affinities of several dienes and their benzene annelated analogues. In most of these compounds the unsaturated groups are sufficiently remote that direct through-space interactions are relatively unimportant, and the splittings observed between the anion states derive from through-bond interactions made possible by mixing of the ethylenic and benzene π^* orbitals with the σ and σ^* orbitals. The ordering of the anion states, like that of the cation states, is found to depend on whether the σ chains contain an even or odd number of bonds.

An important result of this work is the confirmation that laticyclic hyperconjugation is largely responsible for the observed large splittings in the PE spectra of **8** and **16**. Such splittings, if due to the laticyclic hyperconjugation, should be absent in the ETS spectra of **8** and **16** through reasons of symmetry. This indeed is found to be the case.

Electron detachment from the temporary anion states of the compounds studied here is apparently sufficiently fast that sharp structure due to vibrational motion is either absent or very weak. As a result the peaks due to individual anion states are several tenths of an eV broad, making it difficult to determine the splittings between anion states within a few tenths of an eV of one another. We expect that more sophisticated experiments in which the angular distributions of the scattered electrons are measured may be able to "resolve" closely spaced anion states providing they have different symmetries.

It is found that π^*-OIT-n-B decay only slowly with increasing n in both dienes and dibenzo compounds. For dienes the splitting energies are: **3**, 0.8 eV (n = 4); **6**, 0.6 eV (n = 5); and **7**, 0.25 eV (n = 6). The corresponding splitting energies for the dibenzo analogues are somewhat smaller. The data suggest that through-bond interactions between the π^* MO's of two aromatic or ethylenic chromophores are likely to be sizable (i.e., as large as 10^{-3} eV) even when the chromophores are separated by 20 Å. In such a case, through-bond coupling should be sufficiently strong to promote rapid electron transfer over large distances in stable radical anions of compounds such as **31**[13] and **32**.[14]

Acknowledgment. This research was carried out with the support of the National Science Foundation and the Australian Research Grants Scheme. We wish to acknowledge very helpful discussions with Professors P. Burrow and S. Staley.

(60) Waisman, E.; Worry, G.; Marcus, R. A. *J. Electroanal. Chem.* **1977**, *82*, 9.
(61) Hush, N. S. *Trans. Faraday Soc.* **1961**, *57*, 155.
(62) Hush, N. S. *Coord. Chem. Rev.* **1985**, *64*, 135.
(63) Paddon-Row, M. N.; Jordan, K. D. *Mol. Struct. Energet.*, in press.
(64) Assuming a stabilization of the anion states by 1.5 eV due to solvation, which is roughly the degree of stabilization of the anion states of benzene and naphthalene in THF glass, we see that the ground-state anions of **1–10** and their dibenzo analogues should be stable in solution or in glasses. For the dienes the excited π^* anion states may autodetach even for the solvated species, while for the dibenzo compounds, the low-lying excited-state anions are likely to be bound in most cases.